Journal of Medicinal Chemistry

Article

Cite This: J. Med. Chem. XXXX, XXX, XXX−XXX

pubs.acs.org/jmc

Enthalpy-Driven Stabilization of Transthyretin by AG10 Mimics a Naturally Occurring Genetic Variant That Protects from Transthyretin Amyloidosis

Mark Miller,[†] Arindom Pal,[†] Wabel Albusairi,[†] Hyun Joo,[†] Beverly Pappas,[†] Md Tariqul Haque Tuhin,[†] Dengpan Liang,[†] Raghavendra Jampala,[†] Fang Liu,[†] Jared Khan,[†] Marjon Faaij,[†] Miki Park,[†] William Chan,[†] Isabella Graef,[‡] Robert Zamboni,[§] Neil Kumar,[§] Jonathan Fox,[§] Uma Sinha,*[,§] and Mamoun Alhamadsheh*[,†]

[†]Department of Pharmaceutics & Medicinal Chemistry, University of the Pacific, Stockton, California 95211, United States

[‡]Department of Pathology, Stanford University, Stanford, California 94305, United States

[§]Eidos Therapeutics, Inc., San Francisco, California 94101, United States

Supporting Information

ABSTRACT: Transthyretin (TTR) amyloid cardiomyopathy (ATTR-CM) is a fatal disease with no available disease-modifying therapies. While pathogenic TTR mutations (TTRm) destabilize TTR tetramers, the T119M variant stabilizes TTRm and prevents disease. A comparison of potency for leading TTR stabilizers in clinic and structural features important for effective TTR stabilization is lacking. Here, we found that molecular interactions reflected in better binding enthalpy may be critical for development of TTR stabilizers with improved potency and selectivity. Our studies provide mechanistic insights into the unique binding mode of the TTR stabilizer, AG10, which could be attributed to mimicking the stabilizing T119M variant. Because of the lack of animal models for ATTR-CM, we developed an in vivo system in dogs which proved appropriate for assessing the pharmacokinetics−pharmacodynamics profile of TTR stabilizers. In addition to stabilizing TTR, we hypothesize that optimizing the binding enthalpy could have implications for designing therapeutic agents for other amyloid diseases.

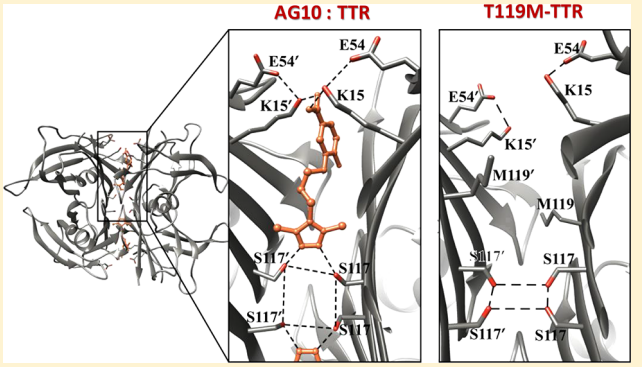

INTRODUCTION

Transthyretin (TTR) amyloidosis (ATTR) is a progressive, fatal disease in which deposition of amyloid derived from either mutant (TTRm) or wild-type (TTRwt) TTR causes severe organ damage and dysfunction.[1,2] Clinically, ATTR presents as cardiomyopathy (ATTR-CM) or peripheral polyneuropathy (ATTR-PN). ATTR-CM is an infiltrative, restrictive cardiomyopathy characterized by progressive left and right heart failure. Familial ATTR-CM (ATTRm-CM) is driven by pathogenic, autosomal dominant, point mutations resulting in amino acid substitutions that destabilize the native TTR tetramer, prompting its dissociation.[3,4] The most prevalent mutation that causes ATTRm-CM is the V122I variant, carried by 3.4% of African Americans, which increases the risk of ATTR-CM several-fold in this population.[5,6] In addition, older individuals may develop ATTR derived from wild-type TTR (ATTRwt-CM). The average life expectancy for people with ATTR-CM is 3−5 years from diagnosis.[7] Unfortunately, ATTR-CM represents one of the largest genetically defined diseases with no approved disease-modifying therapies.

The TTR tetramer features two largely unoccupied thyroxine (T4)-binding sites that are formed between adjacent monomers at the weaker dimer−dimer interface of TTR. Tetramer dissociation into dimers, and then monomers, is the initial and rate-limiting step in TTR amyloidogenesis.[2] The majority of TTR mutations increase the amyloidogenic potential of TTR by lowering its thermodynamic stability and/or decreasing the kinetic barrier for tetramer dissociation.[8] While the V122I variant associated with ATTRm-CM is kinetically destabilized, ATTR-PN is predominantly associated with the thermodynamically destabilized V30M−TTR variant.[9,10]

Two TTR variants, T119M and R104H, have been shown to hyperstabilize heterotetramers composed of these variants and either TTRwt or TTRm, preventing amyloidogenesis in vitro.[9,11] Individuals who are compound heterozygous for both the T119M variant and the polyneuropathy associated V30M−TTR mutation present a more benign evolution of

Received: May 22, 2018

DOI: 10.1021/acs.jmedchem.8b00817
J. Med. Chem. XXXX, XXX, XXX−XXX

Table 1. Comparison of the Binding Affinity, Thermodynamics, and Potency of Stabilizers to TTR in Buffer and Human Serum

		ITC parameters (kcal/mol)					
stabilizer	K_d (nM)	ΔG	ΔH	$T\Delta S$	%TTR occupancy in buffer (1:1 ratio)[a]	%TTR occupancy in serum (2:1 ratio)[a]	%TTR stabilization in serum (2:1 ratio)[a]
AG10	4.8 ± 1.9	−11.34	−13.6	−2.26	79.1 ± 1.2	98.8 ± 2.9	95.4 ± 2.9
tafamidis	4.4 ± 1.3	−11.39	−5.0	6.39	49.9 ± 3.3	49 ± 3.3	41.5 ± 4.6
diflunisal	407 ± 35	−8.72	−8.38	0.34	28.7 ± 0.6	16.2 ± 3.2	24.2 ± 2.3
tolcapone	20.6 ± 3.7	−10.5	−10.1	0.4	71.7 ± 2.5	71.1 ± 2.9	68.4 ± 5.1
1	90 ± 14	−9.61	−9.82	−0.21	58.3 ± 0.9	75.9 ± 3.1	86.7 ± 2.3
2	258 ± 17	−8.99	−6.49	2.5	38.5 ± 0.8	63.2 ± 2.5	70.4 ± 2.2
3	251 ± 12	−9.0	−4.73	4.27	29.7 ± 0.7	43 ± 0.6	32.1 ± 4.9
4	1253 ± 79	−8.1	−2.1	6.0	17.2 ± 0.9	20.8 ± 3.3	23.2 ± 1.1

[a]Stabilizers to TTR ratio. %TTR occupancy in buffer and human serum was determined by FPE assay. %TTR stabilization in human serum was determined by Western blot.

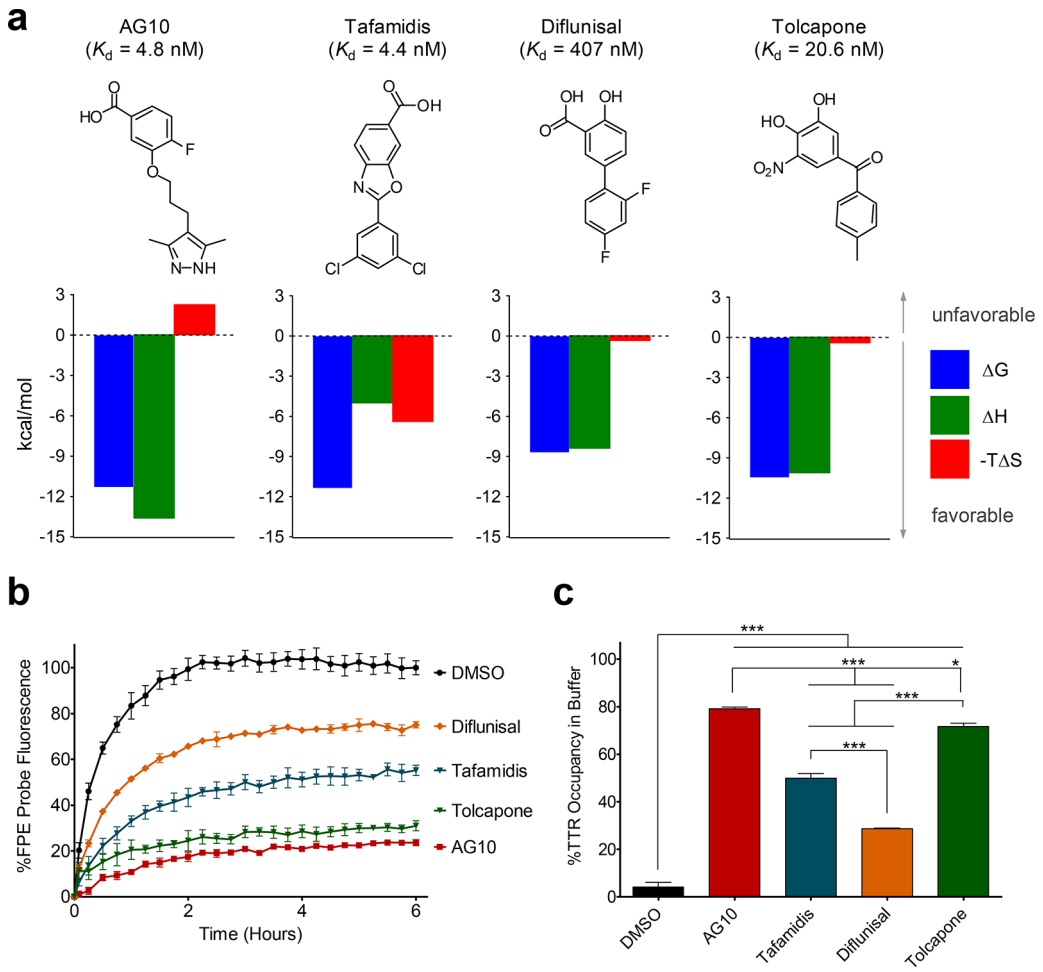

Figure 1. Binding affinities and potency of stabilizers for TTR in buffer. (a) Interaction of TTR with stabilizers assessed by ITC. Thermodynamic data (summarized in Table 1); ΔG are blue bars, ΔH are green bars, and $-T\Delta S$ are red bars. (b) Fluorescence change caused by modification of TTR in buffer (2.5 μM) by FPE probe monitored in the presence of probe alone (control DMSO) or TTR stabilizers (2.5 μM; 1:1 stabilizers to TTR ratio). (c) Bar graph representation of percent occupancy of TTR in buffer by stabilizers in the presence of FPE probe measured after 3 h of incubation relative to probe alone. Error bars indicate SD (n = 3). The significance of the differences were measured by one-way ANOVA followed by Tukey's multiple comparison test (*$p \leq 0.05$; ***$p \leq 0.001$).

ATTR-PN or no disease compared to kindred carrying the V30M−TTR mutation alone.[12] In addition, carriage of the T119M rescue mutation in the absence of other destabilizing TTR mutations has been correlated with a decreased risk of vascular disease and increased life expectancy, as compared to the general (noncarrier) population, by 5−10 years.[13] Similar effects have been described for the R104H−TTR variant in Japanese individuals expressing both R104H and V30M−TTR.[14] The trans-suppressor effects of T119M and R104H are based on different mechanisms.[11] While the T119M kinetically stabilizes the quaternary structure of TTR, the R104H variant is thermodynamically stabilized. Therefore, the stabilizing

DOI: 10.1021/acs.jmedchem.8b00817
J. Med. Chem. XXXX, XXX, XXX−XXX

effect of the T119M mutation is much greater than that of R104H, which only modestly protects against TTR dissociation and aggregation in vitro.

Emerging therapies for ATTR-CM include RNA silencing therapies and TTR stabilizers which are small molecules that bind to the TTR T4 binding sites, thereby stabilizing TTR by increasing the energy barrier of tetramer dissociation.[3] Tafamidis and AG10 are two orally available TTR stabilizers currently in clinical development for ATTR-CM (phase 3 and phase 2, respectively). In addition, diflunisal and tolcapone are two repurposed drugs that have been investigated in ATTR-PN. We have shown earlier that the despite the similar binding affinities (K_d) of AG10 and tafamidis to TTR (K_d = 4.8 ± 1.9 and 4.4 ± 1.3 nM, respectively), AG10 was more potent (in stabilizing TTR in buffer) and more selective for binding and stabilizing TTR in human serum.[15] To account for structural features important for effective TTR stabilization, we performed a side-by-side comparison of the structural, thermodynamic properties, and potency for all ATTR clinical candidates against the crystal structures of stabilizing TTR variants (T119M and R104H). We found that the K_d between a stabilizer and TTR does not correlate well with either potency or selectivity (Table 1). The mechanistic insights gained from our studies suggest that optimizing the enthalpic component of binding plays a crucial if not predominant role in stabilizing TTR. This conclusion was also supported by the synthesis and evaluation of the activity of four new AG10 analogues (compounds **1**, **2**, **3**, and **4**). Several previous studies have shown that enthalpic forces correlated with selectivity of ligands to target proteins including TTR.[16,17] However, there are no reports describing the role of enthalpy in enhancing the potency of ligands in stabilizing multisubunit protein complexes. Our data show that the high potency of AG10 could be attributed to its enthalpically driven binding, mimicking the disease-suppressing properties of the T119M−TTR variant in stabilizing TTR. The potency and selectivity of AG10 for TTR was maintained when AG10 was evaluated in beagle dogs in vivo. To the best of our knowledge, this is the first report describing a correlation between enthalpic binding of a ligand and enhanced potency in stabilizing multiprotein complexes.

RESULTS

Determination of Binding Affinities and Thermodynamics of Interactions Between Stabilizers and TTR. We used isothermal titration calorimetry (ITC) to determine the binding affinities (K_d) and the mechanisms underlying molecular interactions of all TTR stabilizers in clinical development (i.e., AG10, tafamidis, diflunisal, and tolcapone) and AG10 analogues **1**, **2**, **3**, and **4**. Most of the reported TTR ligands bind to the two identical T4 binding sites of TTR with strong negative cooperativity, and therefore the binding of the first ligand will dominate the total binding energy as well as the stabilizing effect. While some differences in cooperativity can be observed in the ITC thermograms, these differences will have minor influences on the binding energy as well as the stabilizing effect. Therefore, the K_d values reported in Table 1 were based on data fitted to an independent single-site binding model.[16] The binding affinities of AG10 and tafamidis to TTR in buffer (K_d = 4.8 ± 1.9 and 4.4 ± 1.3 nM, respectively) were 4-fold higher than tolcapone (K_d = 20.6 ± 3.7 nM) and ∼100-fold higher than diflunisal (K_d = 407 ± 35 nM). The K_d values for compounds **1**−**4** ranged from 90 to 1250 nM, and the results are summarized in Table 1. The K_d for binding of a stabilizer to TTR is represented by the change in Gibbs free energy of binding (ΔG), where $\Delta G = \Delta H - T\Delta S$. By analyzing the thermodynamic signature of each molecule, we can assess the relative contributions of enthalpic (ΔH; representing the formation or breaking of chemical bonds) and entropic forces (ΔS; associated with the amount of disorder in a system and frequently dominated and favored by release of bound water molecule due to hydrophobic interactions). Despite the similar binding affinities of AG10 and tafamidis to TTR in buffer (i.e., similar ΔG values), their binding energetics to TTR are notably different. Whereas the binding of AG10 (ΔH = −13.60 kcal/mol and $T\Delta S$ = −2.26 kcal/mol) is enthalpically driven, tafamidis binding is approximately 50% entropic and 50% enthalpic (ΔH = −5.00 kcal/mol and $T\Delta S$ = 6.39 kcal/mol) (Figure 1a and Table 1). The binding of tolcapone (ΔH = −10.1 kcal/mol and $T\Delta S$ = 0.4 kcal/mol) and diflunisal (ΔH = −8.38 kcal/mol and $T\Delta S$ = 0.34 kcal/mol) is entropically favorable but mainly driven by enthalpic interactions. The unfavorable entropic binding energy of AG10 for TTR ($T\Delta S$ = −2.26 kcal/mol) could be due to its higher polarity and/or conformational flexibility compared to other TTR stabilizers. The themodynamics for the binding interactions between compounds **1**−**4** and TTR is discussed below.

Enthalpic Force Predicts Potency of TTR Stabilizers in Buffer and Efficacy in Human Serum. A recent study with diflunisal and other nonsteroidal anti-inflammatory drugs (NSAIDs) found that ligands with favorable (i.e., larger negative) ΔH had a proportionally higher TTR selectivity compared to ligands with a lower influence of ΔH.[16] While this study described the correlation between enthalpic forces and selectivity of TTR stabilizers, no correlation between binding enthalpy of ligands and potency for stabilizing TTR or, to our knowledge, any other multimeric proteins, has been reported yet. To evaluate the potency of stabilizers in occupying and stabilizing TTR in buffer, we used the fluorescence probe exclusion (FPE) assay.[18] The FPE assay uses a fluorogenic probe (FPE probe, Supporting Information, Figure 1) that is not fluorescent by itself, however, upon binding to the T4 binding site of TTR, it covalently modifies lysine 15 (K15), creating a fluorescent conjugate. Ligands that bind to the T4 site of TTR will decrease FPE probe binding as observed by lower fluorescence. A linear correlation has been reported between the extent of fluorescence in the FPE assay and stabilization of TTR.[18] Therefore, we first used the FPE assay to measure the potency of stabilizers for binding and stabilizing TTR in buffer (tested at 1:1 ratio of stabilizer to TTR tetramer; Figure 1b,c and Table 1). The order of potency of the stabilizers for TTR in buffer was AG10 > tolcapone > tafamidis > diflunisal.

We then employed the FPE and Western blot assays to evaluate the efficacy (representing both potency and selectivity) of stabilizers (10 μM) in occupying and stabilizing TTR in human serum (TTR concentration 5 μM) (Table 1). The Western blot assay measures the amount of intact TTR tetramer after 72 h of acid treatment in the presence and absence of stabilizers. The order of efficacy of the stabilizers in human serum was similar to what we observed for the potency with TTR in buffer (AG10 > tolcapone > tafamidis > diflunisal; Table 1). The potency and efficacy of diflunisal was the lowest which is predicted based on its significantly lower binding affinity to TTR (K_d = 407 ± 35 nM) compared to all

DOI: 10.1021/acs.jmedchem.8b00817
J. Med. Chem. XXXX, XXX, XXX−XXX

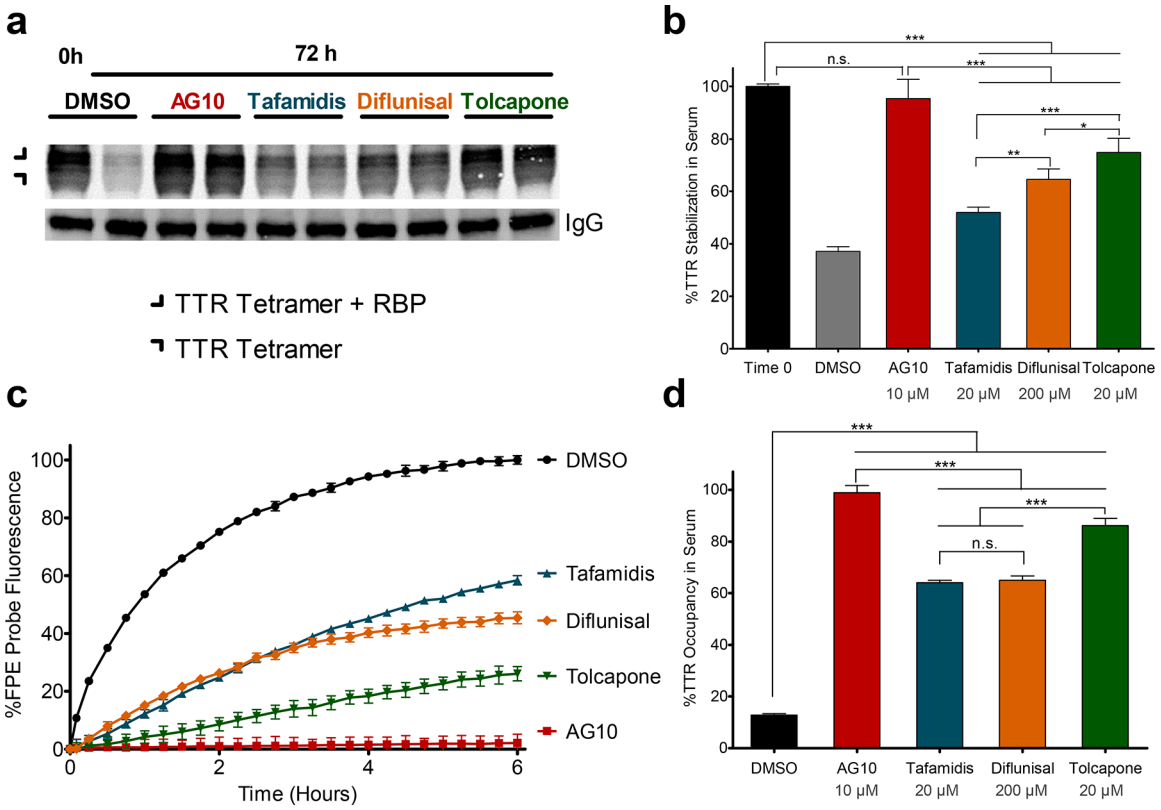

Figure 2. Efficacy of stabilizers in occupying and stabilizing TTR in human serum. (a) Representative Western blot image for the stabilization of TTR in human serum subjected to acid-mediated (pH 4.0) denaturation in the presence of AG10 (10 μM) and other stabilizers tested at their estimated mean clinical C_{max} at steady state when administered at the doses indicated: diflunisal (250 mg bid, 200 μM), tafamidis (80 mg qd, 20 μM), tolcapone (100 mg tid, 20 μM). (b) Bar graph representation of stabilization data obtained from Western blot experiments. Error bars indicate SD (n = 3). (c) Fluorescence change caused by modification of TTR in human serum by FPE probe monitored in the presence of probe alone (control DMSO), AG10 (10 μM), or TTR stabilizers (at their estimated mean clinical steady state C_{max}). (d) Bar graph representation of percent occupancy of TTR in human serum by stabilizers in the presence of FPE probe measured after 3 h of incubation relative to probe alone. Error bars indicate SD (n = 4). The significance of the differences were measured by One-Way ANOVA followed by Tukey's multiple comparison test (n.s., not significant; *$p \leq 0.05$; **$p \leq 0.01$; ***$p \leq 0.001$).

other stabilizers (20−80-fold lower affinity than other stabilizers). Surprisingly, there was no correlation between the K_d values of the three other stabilizers and their potency and efficacy in occupying and stabilizing TTR in both buffer and human serum. For example, the potency and efficacy of tolcapone was higher than that of tafamidis despite the fact that the binding affinity of tolcapone to TTR (K_d = 20.6 ± 3.7 nM) is slightly lower than the binding affinity of tafamidis to TTR (K_d = 4.4 ± 1.3 nM). Interestingly, both potency and efficacy of these stabilizers for TTR in buffer and serum correlated very well (R^2 = 0.98) with their binding enthalpy (ΔH = −13.6, −10.1, and −5.0 kcal/mol; for AG10, tolcapone, and tafamidis, respectively). This data indicate that the enthalpically driven binding of AG10 and tolcapone to TTR (discussed in detail below) is the primary driver of their efficient stabilization of TTR compared to other stabilizers.

We then used the Western blot assay to compare the efficacy of AG10 (10 μM) to other stabilizers at their reported mean maximum plasma concentrations in human (C_{max} of 20 μM for 80 mg tafamidis qd, 200 μM for diflunisal 250 mg bid, and 20 μM for tolcapone 100 mg dose tid). AG10 at 10 μM completely stabilized TTR in human serum (%TTR stabilization: 95.4 ± 4.8%); the other compounds stabilized ∼50−75% of tetrameric TTR at their reported clinical C_{max} (Figure 2a,b). The pK_a values for AG10 (pK_a = 4.13; Supporting Information, Figure 2) and tafamidis (pK_a = 3.73) are higher than that for diflunisal (pK_a = 2.94). Therefore, the percentage ionization of the carboxylic acid groups of stabilizers might vary at pH 4. This could affect the strength of the electrostatic interaction between the carboxylic acid groups and the ϵ-amino groups of lysine 15 (K15) and K15′ at the top of the T4 binding sites which could affect the potency of the stabilizer. To address this concern, we performed the Western blot assay using urea buffer (pH 7.4).[19] The TTR stabilization data of in urea buffer (Supporting Information, Figure 3) is similar to the data obtained from Western blot in acidic pH and from the FPE assay at physiological pH. Consistent with the Western blot TTR stabilization assay data, T4 binding site occupancy by 10 μM AG10 in the FPE assay was essentially complete (%TTR occupancy 96.6 ± 2.1%) and higher than all stabilizers at their reported clinical C_{max}. The target occupancy for tolcapone at 20 μM (%TTR occupancy 86 ± 3.2%) was higher than those of tafamidis and diflunisal (%TTR occupancy ∼65% at 20 and 200 μM, respectively) (Figure 2c,d).

Binding Interactions Between AG10 and S117/S117′ of TTR Mimic Molecular Interactions within the Disease-Protective T119M Mutation. We investigated the correlation between binding enthalpy and TTR stabilization by comparing reported cocrystal structures of stabilizers with

DOI: 10.1021/acs.jmedchem.8b00817
J. Med. Chem. XXXX, XXX, XXX−XXX

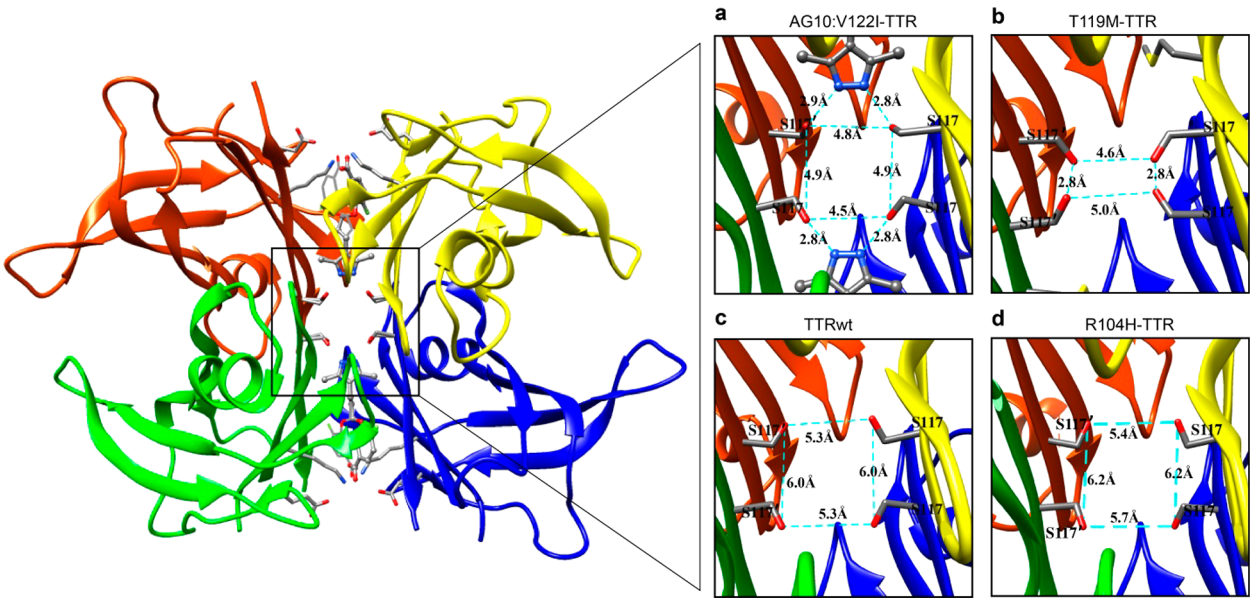

Figure 3. Crystal structures highlighting similar interactions caused by the T119M mutation and binding of AG10 to TTR. (a) Quaternary structure of AG10 bound to V122I−TTR (PDB 4HIQ)[15] shown as a ribbon representation with monomers colored individually. Close-up views of one of the two identical T_4 binding sites with different colored ribbons for the two monomers of the tetramer composing the binding site. Key hydrogen bonds between the pyrazole ring of AG10 and S117/117′ are highlighted by dashed lines. (b) Crystal structure of the stabilizing T119M−TTR variant (PDB 1FHN)[22] with dashed lines highlighting key interactions between the hydroxyl groups of S117 and S117′. (c) Crystal structure of TTRwt (PDB 3CFM).[26] (d) Crystal structure of thermodynamically stabilized R104H−TTR (PDB 1X7T).[27]

TTR against the crystal structures of stabilizing TTR variants (T119M and R104H). We hypothesized that this could allow us to identify functional groups of amino acids within the T4 binding sites of TTR which are important for binding and stabilization of TTR. The carboxylic acid moieties of AG10, tafamidis, diflunisal, and the hydroxyl group on tolcapone all participate in electrostatic interactions with the ε-amino groups of lysine 15 (K15) and K15′ at the top of the T4 binding sites.[15,20,21] The enthalpically driven binding of AG10 and tolcapone to TTR is driven by additional hydrogen bonds that both molecules form within the T4 binding site. The carbonyl group of tolcapone forms one hydrogen bond with hydroxyl side chain of T119 of TTRwt (distance ∼2.6 Å; ideal distance for a hydrogen bond is <3 Å). The longer distance between the carbonyl group of tolcapone and hydroxyl side chain of T119′ on the adjacent monomer (distance ∼7.6 Å) preclude the formation of a second hydrogen bond.[20] Interestingly, this interaction is weaker between tolcapone and V122I−TTR (distance between the carbonyl group of tolcapone and hydroxyl side chains of T119 and T119′ of V122I−TTR are ∼5.5 and ∼9.6 Å, respectively), which could explain the lower binding affinity (K_d = 56 nM) and potency of tolcapone toward V122I−TTR compared to TTRwt.[20] In the case of tafamidis, there is no hydrogen bonding at the base of the T4 pocket; instead, the chlorine atoms of the 3,5-dichloro ring are also placed into halogen binding pocket (HBP) 3 and 3′, where they interact with TTR through predominantly hydrophobic interactions. In addition to electrostatic interactions between the carboxylic acid moiety of AG10 and K15/K15′, AG10 also forms two hydrogen bonds with the hydroxyl side chain serine 117 (S117) and S117′ (distance ∼2.8 Å) of adjacent monomers in the low dielectric macromolecular interior of the T4 binding site (Figure 3a). These additional hydrogen bonds are likely to be responsible for the driving force for the dominant enthalpic binding of AG10 to TTR. Remarkably, similar hydrogen bonds have been reported within the inner cavity of the kinetically stabilizing trans-suppressor T119M−TTR variant (Figure 3b).[22,23]

The two S117 side chain hydroxyl groups of monomers A and B in T119M variant TTR form direct hydrogen bonds with a distance of 2.8 Å, which are not observed in TTRwt (distance between the two S117 residues ∼6.0 Å) (Figure 3c). These unique hydrogen bonds lead to closer contacts between the two dimers (∼4.8 Å) within the TTR tetramer and highlight the potential importance of these hydrogen bonds in the antiamyloidosis and disease-protective effects of the T119M variant on the TTR tetramers. The role of S117 in stabilizing TTR has been also suggested by the binding of flavonoids that are capable of forming a single hydrogen bond with one S117.[24,25] Interestingly, the distance between the S117 and S117′ residues in the thermodynamically stabilized R104H variant, which does not involve kinetic stabilization of the tetrameric TTR, is similar to that of TTRwt (average dimer—dimer distance is ∼5.6 Å, Figure 3c,d).[26,27] The lack of hydrogen bonding between the hydroxyl groups of S117 and S117′ in the R104H variant (which is a less potent trans-suppressor mutant than T119M) highlights the importance of these hydrogen bonds in the antiamyloidogenic and disease suppressing effects of kinetically stabilizing the TTR tetramer in the T119M variant. By forming two direct hydrogen bonds with S117 and S117′ in the TTR tetramer, AG10 creates a similar electrostatic bridge as is found in the protective T119M variant. This data is supported by the analysis of 40 reported crystal structures which highlighted the closer dimer—dimer contacts in the crystal structures of both T119M−TTR (distance ∼4.8 Å) and AG10—V122I−TTR (distance ∼4.66 Å) compared to TTRwt or TTRm (distance ∼5.5 Å) (Supporting Information, Table 1). It is important to note that other known TTR stabilizers do not interact with S117/S117′ of TTR.

DOI: 10.1021/acs.jmedchem.8b00817
J. Med. Chem. XXXX, XXX, XXX−XXX

Scheme 1. Synthesis of AG10 Analogues 1, 2, 3, and 4[a]

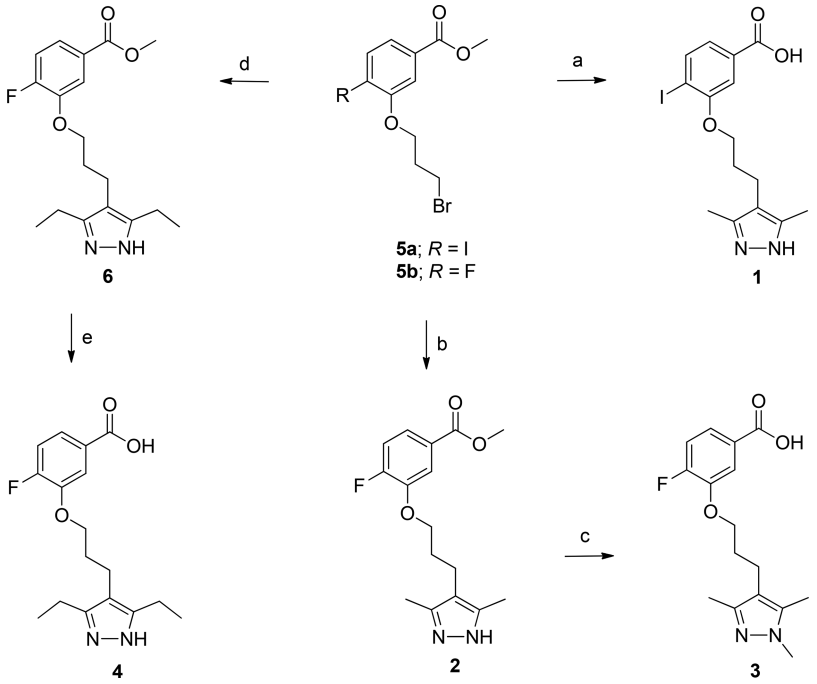

[a](a) **5a**, (i) acetylacetone, DBU, benzene, rt, 3 days, (ii) hydrazine hydrate, ethanol, 90 °C, 4 h, (iii) NaOH, MeOH/water, 50 °C, 14 h; (b) **5b**, (i) acetylacetone, DBU, benzene, rt, 3 days, (ii) hydrazine hydrate, ethanol, 90 °C, 4 h; (c) (i) NaH, MeI, DMF, rt, 12 h, (ii) NaOH, MeOH/water, 50 °C, 14 h; (d) **5b**, (i) 3,5-heptanedione, DBU, benzene, rt, 3 days, (ii) hydrazine hydrate, ethanol, 90 °C, 4 h; (e) NaOH, MeOH/water, 50 °C, 14 h.

Characterization of Key Functional Groups of AG10 Important for TTR Stabilization. To investigate the enthalpic contribution of each of the functional groups of AG10 on TTR binding and stabilization, we synthesized and tested four AG10 analogues (compounds **1**, **2**, **3**, and **4**; Scheme 1) and evaluated their ability to bind and stabilize TTR (Figure 4). AG10 binds TTR with unfavorable entropy ($T\Delta S$ = −2.26 kcal/mol). The fluorine atom of AG10 is placed into HBP1 of TTR, and therefore we hypothesized that the entropic binding of AG10 to TTR could be optimized by replacing the fluorine atom of AG10 with an iodine (compound **1**). Modeling studies suggest the iodine of **1** fits in HBP1 of TTR (where the iodine of T4 binds) which could improve the entropic binding by displacing more water molecules from HBP1 (Figure 4a). Compound **1** displayed significantly lower binding affinity (K_d = 90 ± 14 nM) to TTR in buffer compared to AG10 (K_d = 4.8 ± 1.9 nM). ITC analysis showed that while the entropic interaction of **1** with TTR was more favorable compared to AG10 ($T\Delta S$ = −0.21 and −2.26 kcal/mol, respectively), there was a significant drop in the enthalpic contribution to the binding (ΔH = −9.82 and −13.6 kcal/mol, respectively) (Figure 4b). As suggested by modeling, the decrease in binding enthalpy could be explained by the decrease in strength of the salt bridge between the carboxylic acid moiety of **1** and K15/K15′ (distance ∼4.7 Å compared to ∼2.8 Å for AG10). Compound **1** also displayed reduced potency for TTR in buffer (58.3 ± 0.98%) and human serum (75.9 ± 3.1%) compared to AG10 (Figure 4c−e and Table 1).

The carboxylic acid moiety of AG10 forms two salt bridges directly with the ε-amino groups of K15 and K15′ at the periphery of the T_4-binding site, which serves to close the T_4 pocket around AG10 and partially shield it from the solvent. We synthesized a methyl-ester analogue of AG10 (compound **2**, Figure 4a) to test the effect of modifying the two salt bridges that AG10 forms at the periphery of the T_4-binding site. Compound **2** displayed significantly lower affinity (K_d = 258 ± 17 nM) to TTR in buffer compared to AG10 (K_d = 4.8 ± 1.9 nM), which could be explained by the lower strength of potential hydrogen bonds between the ester group of **2** and K15/K15′ (ΔH = −6.49 kcal/mol) compared to the salt bridge in AG10 (Figure 4b). Compound **2** also displayed reduced potency for TTR in buffer and human serum compared to AG10 and compound **1** (Figure 4c−e and Table 1).

The 3,5-dimethyl-1*H*-pyrazole ring of AG10 sits deep within the inner cavity of the T_4-binding site and forms two hydrogen bonds with the S117 and S117′ of adjacent subunits.[15] By blocking these interactions, we can effectively observe their enthalpic contribution using ITC and the FPE assay, respectively. Therefore, we synthesized compound **3** which has an *N*-methyl pyrazole. The *N*-methyl group would restrict the pyrazole ring of **3** to form only one hydrogen bond with one of the adjacent TTR subunits (Figure 4a). We also synthesized compound **4** where the dimethyl pyrazole of AG10 was replaced with diethyl pyrazole. Modeling studies suggested that the bulk of the diethyl groups would prevent the molecules for reaching deep in the T_4-binding site, thereby decreasing its ability to potentially form any hydrogen bonds with S117/S117′ (Figure 4a). As predicted by modeling, both **3** (K_d = 251 ± 12 nM) and **4** (K_d = 1253 ± 79 nM) showed greatly reduced binding affinity to TTR in buffer. This reduced affinity was translated into a significant decrease in potency for TTR in buffer and human serum, especially for compound **4**. The order of potency for stabilizing TTR was similar in both buffer and serum (**1** > **2** > **3** > **4**; Figure 4c−e and Table 1). As

DOI: 10.1021/acs.jmedchem.8b00817
J. Med. Chem. XXXX, XXX, XXX−XXX

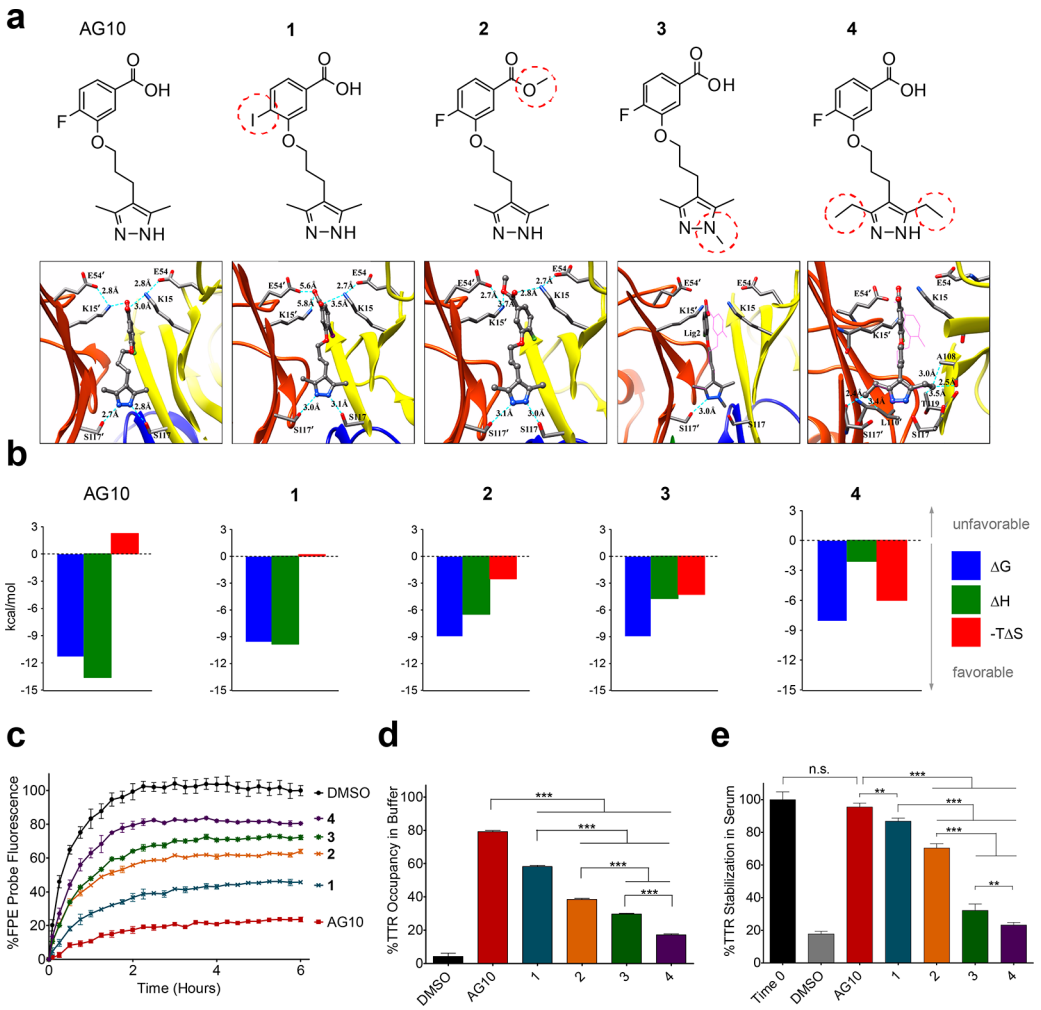

Figure 4. Hydrogen bonds between the pyrazole ring of AG10 and S117/S117′ of TTR are important for effective binding to TTR. (a) Chemical structures and in silico docking study of synthesized AG10 analogues **1**, **2**, **3**, and **4**. Co-crystal structure of AG10 bound to TTR used for the docking experiment. **1** is the iodo-analogue of AG10. **2** is the methyl-ester form of AG10 that cannot form salt bridge with K15/15′. **3** is the methyl-pyrazole form of AG10 that can potentially form only one hydrogen bond with either K15 or K15′. **4** is the diethyl-pyrazole analogue of AG10 which affects both hydrogen bonds with S117/S117′. (b) Interaction of TTR with analogues assessed by ITC. Thermodynamic data; ΔG are blue bars, ΔH are green bars, and $-T\Delta S$ are red bars. (c) Fluorescence change caused by modification of TTR in buffer (2.5 μM) by FPE probe monitored in the presence of probe alone (control DMSO) or TTR stabilizers (2.5 μM; 1:1 stabilizers to TTR ratio). (d) Bar graph representation of percent occupancy of TTR in buffer by stabilizers in the presence of FPE probe measured after 3 h of incubation relative to probe alone. Error bars indicate SD (n = 3). (e) Bar graph representation of Western blot data for the stabilization of TTR in human serum by analogues (10 μM; 2:1 stabilizers to TTR ratio). Error bars indicate SD (n = 4). The significance of the differences were measured by one-way ANOVA followed by Tukey's multiple comparison test (n.s., not significant; *$p \leq 0.05$; **$p \leq 0.01$; ***$p \leq 0.001$).

we observed with the clinical ATTR stabilizers, the potency of AG10 and compounds **1**, **2**, **3**, and **4** in occupying and stabilizing TTR correlated very well (R^2 = 0.98) with the binding enthalpy of these molecules (ΔH = −13.6, −9.82, −6.49, −4.73, and −2.1 kcal/mol, respectively). Interestingly, despite the similar binding affinities of **2** and **3**, their potency was significantly different (Table 1). The higher potency of **2** compared to **3** could be explained by its favorable enthalpic binding (ΔH = −6.49 and −4.73 kcal/mol, respectively) (Figure 4b). This observation is similar to the data obtained for AG10 and tafamidis (i.e., similar K_d values but significantly different potency) (Table 1). These results highlight the crucial role played by the pyrazole ring and the importance of the hydrogen bonds it forms with the two TTR dimers, mimicking the interactions in the protective T119M−TTR mutation and enhancing the kinetic stability of the TTR tetramer.

Examining the Effect of Enthalpy on the Selectivity of AG10 to TTR. To examine the role of enthalpy on the selectivity of AG10 for TTR over other abundant serum proteins, we tested the concentration−effect relationship of AG10 and tafamidis in the FPE assay in whole human serum (Supporting Information, Figure 4a,b). We tested AG10 and tafamidis because their binding affinities for TTR in buffer is very similar (K_d = 4.8 ± 1.9 and 4.4 ± 1.3 nM, respectively) but their thermodynamics for binding TTR, especially the enthalpy component, is significantly different. Therefore, the data obtained in serum would largely reflect selectivity. AG10 displayed a progressive concentration-dependent occupancy, with complete occupancy achieved at AG10 concentrations ≥10 μM. Even at substoichiometric concentrations, AG10 was able to occupy and stabilize the majority of TTR (at 5 μM, TTR occupancy of 69.2% by FPE, 74.5% stabilization by Western blot). In contrast, there was a more modest increment

DOI: 10.1021/acs.jmedchem.8b00817
J. Med. Chem. XXXX, XXX, XXX−XXX

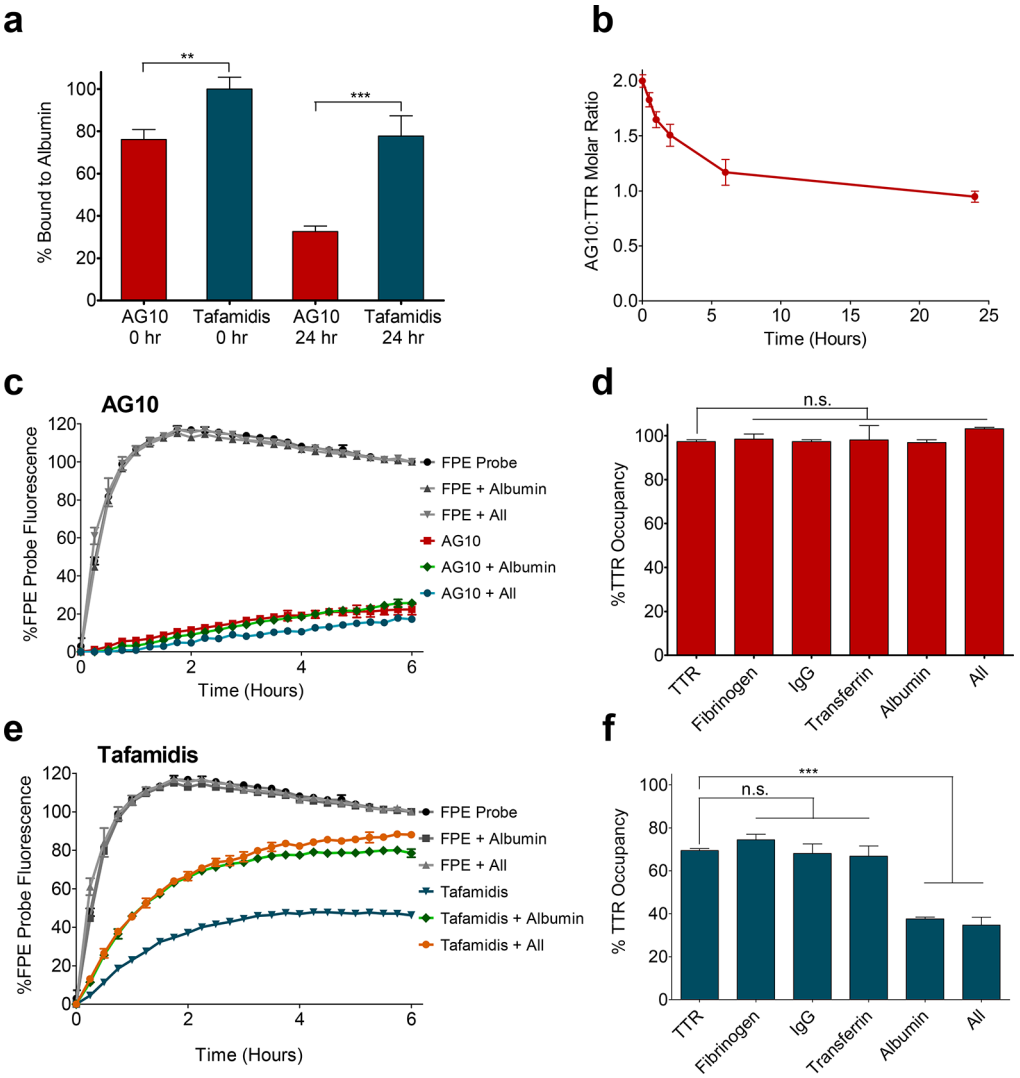

Figure 5. AG10 has high selectivity for binding TTR over albumin or other abundant human serum proteins. (a) Gel filtration and dialysis assay comparing AG10 and tafamidis (each at 30 μM) incubated with purified human serum albumin (600 μM). The concentration of tafamidis bound to albumin after gel filtration (i.e., dialysis time 0 h) was normalized to 100%. Error bars indicate SD (n = 3). (b) 24 h time-course for dialysis of AG10 (10 μM) incubated with purified human TTR (5 μM). Error bars indicate SD (n = 3). (c) Fluorescence change due to modification of purified human TTR (5 μM) by FPE probe monitored for 6 h in the presence of probe alone (black circles), probe plus albumin (600 μM) (black triangles), probe plus all [fibrinogen (5 μM), albumin (600 μM), IgG (70 μM), transferrin (25 μM)] (gray triangles), probe and AG10 (10 μM) (red squares) or probe and AG10 plus albumin (green diamonds), and probe and AG10 plus all [fibrinogen (5 μM), albumin (600 μM) IgG (70 μM), transferrin (25 μM)] (blue circles). (d) %TTR occupancy in buffer by AG10 in the presence of FPE probe and other serum proteins measured after 3 h of incubation relative to probe alone. (e,f) Same experiment described for AG10 was performed for tafamidis. Error bars indicate SD (n = 3). The significance of the differences were measured by One-Way ANOVA followed by Tukey's multiple comparison test (n.s., not significant; *$p \leq 0.05$; **$p \leq 0.01$; ***$p \leq 0.001$).

in either occupancy or stabilizing activity of tafamidis at concentrations above 20 μM (Supporting Information, Figure 4c,d). A good correlation (R^2 = 1.0) between TTR occupancy (by FPE) and TTR stabilization (by Western blot) was observed when the activity of AG10 was evaluated (Supporting Information, Figure 5a,b). For tafamidis, there was a good correlation (R^2 = 0.87) for concentrations up to 10 μM, however, at higher concentrations, there was a plateau in the FPE assay (Supporting Information, Figure 5c,d).

The selectivity of AG10 and tafamidis for TTR was further investigated by repeating these assays in buffer in the presence or absence of purified serum proteins. AG10 or tafamidis (30 μM) were preincubated with purified human serum albumin (at its physiological concentration of 600 μM) and then subjected to gel filtration followed by dialysis. At time 0 (immediately after gel filtration), less AG10 was bound to albumin compared to tafamidis (18.3 ± 0.98 vs 24.1 ± 1.1 μM; Figure 5a). Following dialysis vs buffer for 24 h, the concentration of AG10 bound to HSA was lower than that for tafamidis (7.8 ± 0.1 vs 18.8 ± 2.1 μM). These data indicate that AG10 has a lower binding affinity for albumin compared to tafamidis. In parallel, the binding of AG10 to TTR was also investigated in this gel filtration/dialysis assay. AG10 (10 μM) was preincubated with an equimolar ratio TTR (5 μM of tetrameric TTR, representing 10 μM of TTR T4 binding sites). The dissociation of AG10 from TTR was slow for the first six hours (AG10−TTR molar ratio of ∼1.2:1) and

DOI: 10.1021/acs.jmedchem.8b00817
J. Med. Chem. XXXX, XXX, XXX−XXX

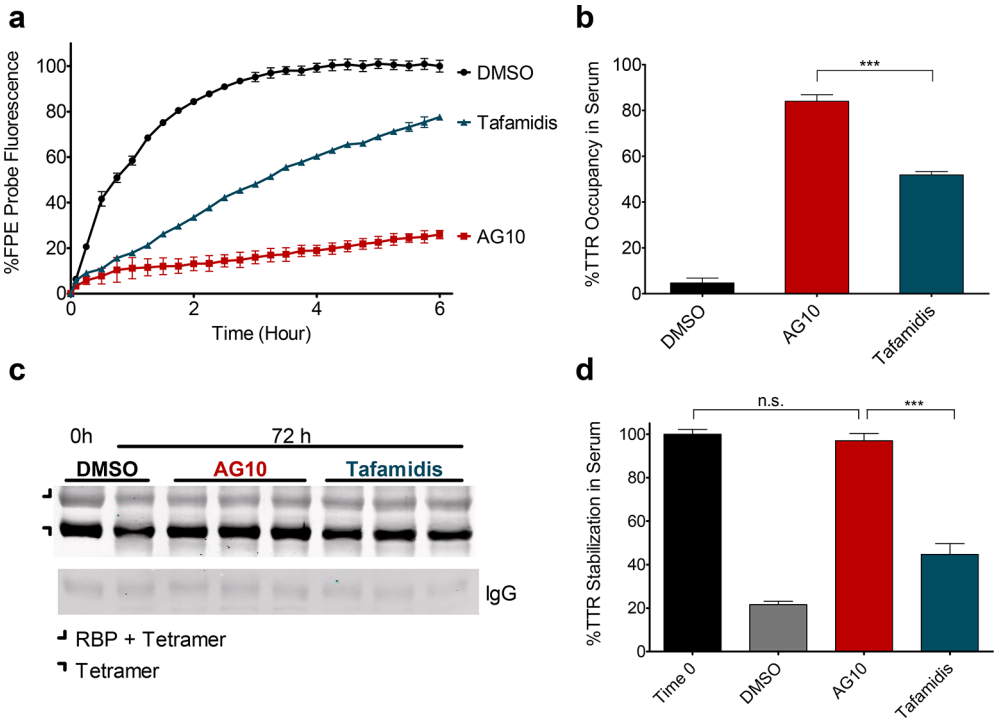

Figure 6. Activity of AG10 and tafamidis in the FPE and Western blot assays performed with pooled dog serum. (a) Fluorescence change caused by modification of dog TTR in commercially available beagle dog serum by FPE probe monitored in the presence of probe alone (control DMSO, black circles), AG10 (10 μM) or tafamidis (10 μM). (b) Percent occupancy of dog TTR in dog serum by AG10 and tafamidis in the presence of FPE probe measured after 3 h of incubation relative to probe alone. Error bars indicate SD (n = 4). (c) Western blot image for the stabilization of TTR in pooled dog serum against acid-mediated denaturation in the presence of AG10 (10 μM) and tafamidis (10 μM). Serum samples were incubated with DMSO or test compounds in acetate buffer (pH 4.0) for the desired time period (0 and 72 h) before cross-linking and immunoblotting. (d) Bar graph representation of stabilization data obtained from Western blot experiments. Error bars indicate SD (n = 3). The significance of the differences were measured by One-Way ANOVA followed by Tukey's multiple comparison test (n.s., not significant; *$p \leq 0.05$; **$p \leq 0.01$; ***$p \leq 0.001$)

maintained a 1:1 molar ratio over a 24 h incubation (Figure 5b).

Finally, the selectivity of AG10 and tafamidis for binding to TTR in human serum was evaluated using a modified FPE assay where human serum was replaced with purified human TTR in buffer (PBS buffer, pH 7.4). In addition to purified TTR (5 μM), four separate representative and abundant plasma proteins were added to the FPE assay in buffer. Addition of albumin, transferrin, fibrinogen, or immunoglobulin (IgG) did not influence TTR occupancy by AG10 (>97% TTR occupancy in the absence or presence of any of these proteins, Figure 5c,d). Albumin, but not the other serum proteins tested, interfered with TTR occupancy by tafamidis (41.5 ± 0.9% vs 68.2 ± 0.1% in the absence of albumin; Figure 5e,f). Adding all of the tested plasma proteins simultaneously yielded identical results for AG10. The higher selectivity of AG10 for TTR could be attributed to a number of properties, including the enthalpic binding and greater hydrophilicity of AG10 (ClogP = 2.78) compared to the more lipophilic tafamidis (ClogP = 4.2).

Healthy Beagle Dog is a Suitable Experimental Model for Evaluating the Efficacy of TTR Stabilizers. We then investigated if the high potency and selectivity of AG10 for TTR can be maintained in vivo. Transgenic animal models that faithfully reproduce the pathology of human ATTR-CM are not yet available. Therefore, we took an approach similar to that currently used in the clinic to examine the efficacy of AG10 vs other TTR kinetic stabilizers. The activity of TTR stabilizers in occupying and stabilizing TTR is commonly assessed ex vivo in blood samples obtained from patients before and after dosing of the stabilizer. To explore the in vivo activity of AG10, this same approach was used in the healthy beagle dog. The healthy beagle dog was chosen as an experimental model for several reasons. All amino acids in the T4 binding sites of TTR, where AG10 and other stabilizers bind, are conserved between dog and human.[28] We also tested the concentration of TTR in dog serum (~4.6 μM) and found it similar to that of healthy humans (Supporting Inforemation, Figure 6).

To confirm the suitability of assays used with human-based reagents for dog studies, the activity of AG10 and tafamidis was evaluated in pooled dog serum using the same FPE and Western blot assays used for the experiments described above. The in vitro TTR binding and stabilization concentration–effect relationships of AG10 and tafamidis in both assays repeated using dog serum was similar to those observed in human serum (Figure 6). These features made the healthy canine a suitable system for subsequent investigations.

AG10 Potently and Selectively Binds to Canine TTR Following Oral Administration. To explore the pharmacokinetic–pharmacodynamic (PK–PD) relationship in vivo, AG10 was administered to healthy beagle dogs daily by oral gavage for 7 days. A total of 16 male (M) and 16 female (F) beagle dogs made up four treatment groups: (i) 6M/6F at 0 mg/kg/d (vehicle control), (ii) 2M/2F at 50 mg/kg/d, (iii) 2M/2F at 100 mg/kg/d, and (iv) 6M/6F at 200 mg/kg/d.

DOI: 10.1021/acs.jmedchem.8b00817
J. Med. Chem. XXXX, XXX, XXX–XXX

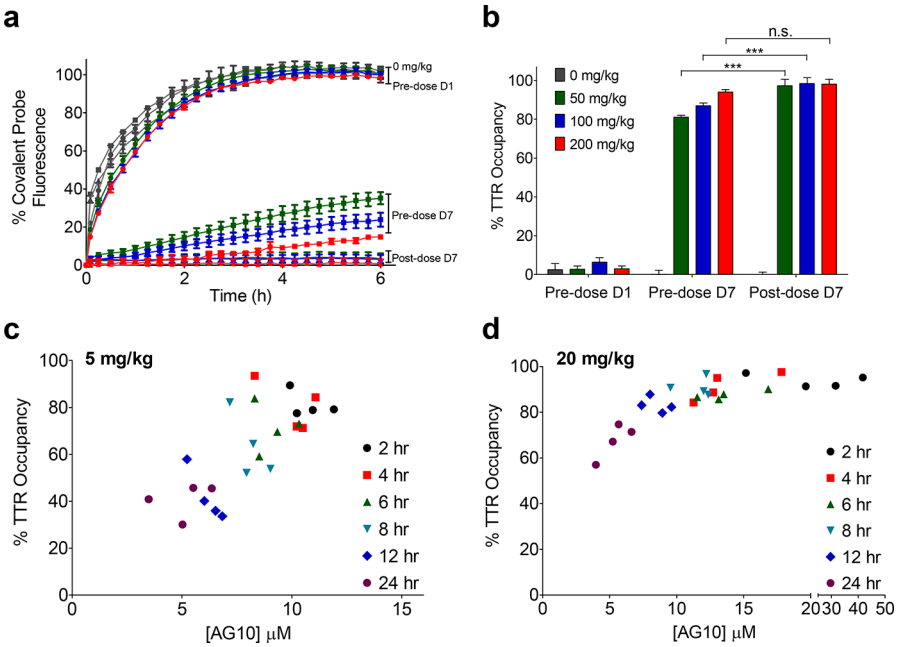

Figure 7. Orally administered AG10 is effective in binding and stabilizing TTR in dogs. (a,b) Occupancy of TTR in beagle dogs after oral administration (qd for 7 days) of escalating doses of AG10. Circles (●) indicate predose day 1, squares (■) indicate predose day 7 (AG10 concentration at C_{min}), and triangles (▲) indicate postdose day 7 (AG10 concentration at C_{max}). Four groups of animals were dosed: (i) 0 mg/kg (n = 12, 6 males/6 females), (ii) 50 mg/kg (n = 4, 2 males/2 females), (iii) 100 mg/kg (n = 4, 2 males/2 females), and (iv) 200 mg/kg (n = 12, 6 males/6 females). (b) Bar graph representing TTR occupancy at 3 h. Error bars indicate SD (n = 3). (c,d) Pharmacokinetic−pharmacodynamic (PK−PD) analysis of AG10 in dogs receiving a single oral dose of AG10 at (c) 5 mg/kg and (d) 20 mg/kg. Scatterplot of concentration [AG10] vs %TTR occupancy of serum samples obtained from dogs at various time points (n = 4, 2 males/2 females per dosing group). Error bars indicate SD (n = 3). The significance of the differences were measured by One-Way ANOVA followed by Tukey's multiple comparison test (n.s., not significant; *$p \leq 0.05$; **$p \leq 0.01$; ***$p \leq 0.001$).

Timed serum samples were collected predose on study day 1 (baseline), predose on study day 7 (representing trough concentrations, or C_{min}, at steady state), and at 1 h postdose on study day 7 (representing peak concentrations, or C_{max}, at steady state). Binding occupancy of TTR by AG10 was assessed by FPE assay (Figure 7a,b). All samples from dogs treated with vehicle alone, and those collected from the active treatment arms prior to exposure to AG10, showed zero TTR occupancy. Serum from AG10-treated dogs displayed a dose-proportional response in binding occupancy at the steady state trough (day 7 predose; ∼81−94% TTR occupancy), and all AG10 treated groups showed complete (>97%) TTR occupancy at steady state C_{max} (day 7 postdose). Lower doses of AG10 were subsequently tested to further explore the PK−PD (exposure−effect) relationship in order to identify a minimally effective dose of AG10 that might still effectively bind to and stabilize TTR. Eight dogs divided into two active treatment groups received either 5 or 20 mg/kg AG10 as a single oral dose. These results showed enhanced TTR occupancy in the 20 vs 5 mg/kg dose groups (Figure 7c,d, and Supporting Information, Figure 7). The %TTR occupancy at C_{max} was significantly higher ($p \leq 0.001$) than at C_{min} for both doses. There was significantly higher ($p \leq 0.001$) TTR occupancy for the 20 mg/kg dose compared to the 5 mg/kg dose at C_{min}. The data also showed that circulating plasma concentration of AG10 correlates well with %TTR occupancy.

■ DISCUSSION

Optimizing the binding enthalpy of small molecules has been associated with the development of second-generation drugs with improved selectivity.[16,17,29] Enthalpic forces have also been correlated with the stability of protein association complexes.[30,31] However, the effect of the enthalpic component of binding of a small molecule on its potency in stabilizing multimeric proteins has not been reported. To account for structural features important for effective TTR stabilization, we compared the TTR binding and stabilizing activity of four ATTR clinical candidates and four AG10 analogues. We found that the K_d between a stabilizer and TTR does not by itself correlate well with either potency or selectivity (Table 1). Our results suggest that enthalpic forces, in combination with K_d measurements in a purified protein, are better predictors of both potency and selectivity for stabilizing TTR in serum.

The trans-suppressor T119M−TTR is a superstabilizing variant compared to TTRwt (reported T119M−TTR dissociation rate is 40-fold slower than that of TTRwt).[9] This variant effectively ameliorates disease progression and symptoms in compound heterozygous individuals carrying the pathogenic, destabilizing V30M mutation.[12] The T119M substitution induces conformational changes that promote hydrogen bonding between the hydroxyl groups of adjacent S117 residues of T119M−TTR monomers and lead to closer contacts between the two dimers within the tetramer.[22] These enthalpically favorable interactions and their consequences are neither observed in TTRwt nor in the thermodynamically stabilized, disease-protective R104H variant, suggesting that they are important for the enhanced kinetic stabilization of the TTR tetramer. Our studies show that AG10s enthalpically driven mode of action is through kinetic stabilization of TTR, which is similar to the kinetically stabilizing T119M variant and not comparable to the thermodynamically stabilizing

DOI: 10.1021/acs.jmedchem.8b00817
J. Med. Chem. XXXX, XXX, XXX−XXX

R104H. When comparing the T119M mutation to the cocrystal structure of AG10 bound to the kinetically destabilized V122I−TTR, the similarities of these critical intramolecular interactions are evident and we conclude that AG10s mode of binding, especially the two hydrogen bonds with S117/S117′ that are buried in the low dielectric macromolecular interior of the T4 pocket, may well explain AG10s efficient binding and stabilizing of tetrameric TTR. The experiments comparing closely related, structural analogues of AG10 highlight the important role of the pyrazole ring of AG10 in enthalpically driving the binding by forming two hydrogen bonds with different subunits of TTR. These unique interactions with the S117/S117′ residues at the bottom of the T4 binding pocket of TTR are not observed in other stabilizers. To the best of our knowledge, this is the first report describing a correlation between enthalpic binding of a ligand and enhanced potency in stabilizing multiprotein complexes.

Similar to T119M−TTR, enthalpic forces have been reported to play a dominant role in stabilizing the eye lens crystallin proteins. Analysis of the association energetics of β-crystallins (which associate into dimers, tetramers, and higher order oligomers) showed that β-crystallins which associate by predominately hydrophobic forces participate in a weaker protein associations whereas the formation of stable tetramers is dominated by enthalpically driven interactions between the subunits (mediated by hydrogen bonds, salt bridges, and van der Waals interactions).[32] Hereditary cataracts are caused by mutations that destabilize the crystallin proteins, leading to the assembly of crystallins into amyloid-like fibers. For example, the R120G mutation in αB-crystallin disrupts ionic interactions that normally stabilize the αB-crystallin dimer (wild-type αB-crystallin dimer is stabilized by a salt bridge between R120 and D109).[33] These studies with TTR (where the introduction of an enthalpic interaction in the T119M variant hyperstabilize the tetramer) and crystallins (where disrupting an enthalpic interaction in the R120G variant destabilizes the dimer) suggest that enthalpic forces controlling protein association could be similar to forces influencing effective protein stabilization by small molecules such as AG10. This hypothesis would be further supported by additional site-directed mutagenesis and structural studies to investigate if factors other than enthalpy are also involved in the enhanced stabilization of TTR.

CONCLUSIONS

In summary, we have developed a preclinical in vivo approach to evaluate the efficacy of TTR stabilizers. Beagle dogs demonstrated that AG10 is orally available and achieves dose-dependent plasma concentrations that potently and selectively bind and stabilize tetrameric TTR. The similarity between dog and human TTR and the expected similarity in PK behavior of many small molecules between dog and human, suggest that these data can serve as a guide for selecting a dosing regimen for stabilizers to attain safe and effective TTR binding and stabilization in ATTR-CM patients. By analyzing the molecular interactions that stabilizers form with TTR and comparing it to interactions within stabilizing TTR mutations, we suggest that electrostatic interactions formed deep in the T4 site of TTR (which could be similar to the hydrogen bonds between S117/117′ of T119M−TTR and between the pyrazole of AG10 and TTR) are more effective in stabilizing TTR compared to hydrophobic interaction and interactions at the solvent exposed portion of the T4 pocket. There are limited examples where the binding of a small molecule to a known disease-causing target mimics a stabilizing mutation identified in that target protein.[34] In addition to stabilizing TTR, we hypothesize that molecules with similar enthalpically driven binding mode to that of AG10 could be useful in stabilizing multisubunit protein complexes in certain diseases such as crystallins in cataract and α-synuclein tetramer in Parkinson's disease.[35,36]

EXPERIMENTAL SECTION

Experimental Animals. All experiments with male and female beagle dogs were conducted in accordance with National Institutes of Health guidelines for the care and use of live animals and were approved by the Institutional Animal Care and Use Committee of Covance and PreClinical Research Services.

Isothermal Titration Calorimetry (ITC). Binding experiments were performed using MicroCal PEAQ-ITC at 25 °C. A solution of ligand (25 μM in PBS pH 7.4, 100 mM KCl, 1 mM EDTA, 2.5% DMSO) was prepared and titrated into an ITC cell containing 2 μM of TTR in an identical buffer. Nineteen injections of ligand (2.0 μL each) were injected into the ITC cell (at 25 °C) to the point that TTR was fully saturated with ligand. Calorimetric data were plotted and fitted using the standard single-site binding model. For control, we tested the enthalpy change caused by titrating bank DMSO in buffer into TTR and the resulting binding enthalpy was <0.4 kcal/mol. We also used ITC to titrate tafamidis and AG10 against human serum albumin (HSA). The K_d value for tafamidis (2.3 μM) was similar to what has been reported earlier (K_d = 2.5 μM; EMA assesment report EMA/729083/2011). The binding affinity of AG10 was calculated around 8 μM, which also fits with our data in Figure 5 (where AG10 has lower binding to albumin compared to tafamidis).

FPE Assay for Binding TTR in Buffer and Human or Dog Serum. The binding affinity and selectivity of AG10 and other stabilizers to TTR in buffer and serum was determined by their ability to compete with the binding of a fluorescent probe exclusion (FPE probe) binding to TTR in buffer and human serum.[18] The FPE probe is a thioester TTR ligand (Supporting Information, Figure 1) that is not fluorescent by itself, however, upon binding to the T4 binding site of TTR, it covalently modifies lysine 15 (K15), creating a fluorescent conjugate. Ligands that bind to the T4 site of TTR will decrease FPE probe binding as observed by lower fluorescence. The FPE assay was also adapted for use with dog serum. *FPE with TTR in buffer:* An aliquot of 98 μL of TTR in PBS (pH 7.4, final concentration 2.5 μM) was mixed with 1 μL of test compounds (2.5 μM) and 1 μL of FPE probe (0.18 mM stock solution in DMSO; final concentration 1.8 μM). The change in fluorescence (λ_{ex} = 328 nm and λ_{em} = 384 nm) were monitored using a microplate spectrophotometer reader (SpectraMax M5) for 6 h at rt. *FPE with TTR in human and dog serum:* An aliquot of 98 μL of pooled human serum (prepared from human male AB plasma, Sigma; catalogue no. H4522; TTR concentration 5 μM) or dog serum (Innovative Research, catalogue no. IBG-SER; TTR concentration 4.6 μM) was mixed with 1 μL of test compounds [all compounds were prepared as 10 mM stock solutions in DMSO and diluted accordingly with DMSO (final concentrations in serum were AG10 10 μM; diflunisal 200 μM; tafamidis 20 μM; tolcapone 20 μM)] and 1 μL of FPE probe (0.36 mM stock solution in DMSO; final concentration 3.6 μM). In the case of dog serum (after oral treatment with AG10), 1 μL of FPE probe and 1 μL of DMSO were added to each well and mixed with 98 μL of the appropriate dog serum sample. The change in fluorescence (λ_{ex} = 328 nm and λ_{em} = 384 nm) were monitored using a microplate spectrophotometer reader (SpectraMax M5) for 6 h at rt.

Stability Studies of TTR in Serum by Immunoblotting. Western blotting was performed as reported earlier.[15,37] All compounds were prepared as 10 mM stock solutions in DMSO and diluted accordingly with DMSO (final concentrations in serum were: AG10 10 μM, diflunisal 200 μM, tafamidis 20 μM, tolcapone 20 μM). Then 2 μL of each compound were added to 98 μL of human serum (TTR concentration 5 μM). The samples were incubated at 37 °C for

DOI: 10.1021/acs.jmedchem.8b00817
J. Med. Chem. XXXX, XXX, XXX−XXX

2 h, and then 10 μL of the samples were diluted 1:10 with acidification buffer (pH 4.0, 100 mM sodium acetate, 100 mM KCl, 1 mM EDTA, 1 mM DTT). The Western blot assay was also performed in urea buffer (pH 7.4) as reported earlier.[19] The samples were incubated at room temperature for 72 h, cross-linked with glutaraldehyde (final concentration of 2.5%) for 5 min, and then quenched with 10 μL of 7% sodium borohydride solution in 0.1 M NaOH. All samples were denatured by adding 100 μL of SDS gel loading buffer and boiled for 5 min. Then 10 μL of each sample was separated in 12% SDS-PAGE gel and analyzed by immunoblotting using anti-TTR antiserum (DAKO A0002, 1:10000 dilution for human serum and 1:2000 for dog serum). The combined intensity of TTR bands (TTR tetramer and tetramer bound to RBP) was quantified by using an Odyssey IR imaging system (LI-COR Bioscience) and reported as percentage of TTR tetramer relative to TTR tetramer density of DMSO control at 0 h (considered 100% stabilization) and 72 h (ranges between 10% and 35% TTR remaining). The percentage tetramer stabilization is calculated as 100 × [(tetramer and tetramer + RBP density, 72 h)/(tetramer and tetramer + RBP density of DMSO, 0 h)].

In Silico Structural and Modeling Studies. The analyses of the crystal structures of TTR were carried out on four TTR crystal structures obtained from the RCSB PDB site. Biological assemblies of TTR tetramers were constructed using the X-ray crystallographic unit cell information given in the pdb files. When multiple models were suggested, the first choice model was used. The initial geometries of the AG10 and its four derivatives (**1**, **2**, **3**, and **4**) built with Molden[38] were used, and geometry optimizations were carried out at the hybrid density functional B3LYP level with 6-311+G(d) basis set using the Gaussian'09 program package (Wallingford, CT, USA; Gaussian, Inc., 2009). The Frequency calculations on the optimized geometries were carried out to ensure they have no imaginary frequencies. Dock 6 program was used for the docking experiments. The crystal structure of the V122I mutant TTR complex with AG10 (PDB 4HIQ)[15] was used as the receptor. Tetrameric TTR was built using the crystallographic data, solvent and other heteroatoms were removed, and one large docking grid was selected including the T4 binding sites. For all the docking experiments, the same receptor and the grid were used. The flexible ligand docking was carried out to allow the rotation around the torsion angles. UCSF Chimera package was used in visualization and analyses of the 3D structures.[39]

Binding of AG10 and Tafamidis to Human Serum Albumin. Test compounds (AG10 or tafamidis; both at 30 μM) were incubated with human serum albumin (HSA, 600 μM; albumin from human serum; Sigma-Aldrich, catalogue no. A3782) in assay buffer (10 mM sodium phosphate, 100 mM KCl, and 1 mM EDTA, pH 7.6) for 1 h at 37 °C. Then 500 μL of a solution of HSA and AG10 or tafamidis mixture in assay buffer was subjected to gel filtration on PD Minitrap G25 columns (GE Life Sciences, catalogue no. 45-001-529) by gravity and the fractions containing HSA were identified by NanoDrop. The concentration of HSA (i.e., concentration at time zero) was also determined using NanoDrop (based on calibration curves of known HSA concentrations). HSA concentration was 351 μM for the tafamidis sample and 345 μM for AG10 sample. The concentration of test compounds in these fractions (i.e., concn at time zero) was evaluated using HPLC (based on calibration curves of known concentration of test compounds). Then 500 μL of each HSA/test compound samples was then added to a Slide-A-Lyzer dialysis cassette G2 (3.5K MWCO, Thermo Scientific, catalogue no. PI87722). The dialysis cassettes were placed in 100 mL of assay buffer and stirred at room temperature. After 24 h, the samples were removed from dialysis cassette and the volume was measured. The concentration of HSA and test compounds were determined using NanoDrop and HPLC as described above.

Dialysis of AG10:TTR Complex. AG10 (10 μM) was incubated with human wild-type TTR (5 μM, purified from human plasma; Sigma-Aldrich, catalogue no. P1742) in assay buffer (10 mM sodium phosphate, 100 mM KCl, and 1 mM EDTA, pH 7.6) for 1 h at 37 °C. Then 500 μL of each AG10/TTR solution was then added to a Slide-A-Lyzer dialysis cassette G2. The dialysis cassettes were placed in 100 mL of assay buffer and stirred at room temperature. Samples from the dialysis buffer were taken at different time points (0, 0.5, 1, 2, 6, and 24 h). After 24 h, the samples were removed from dialysis cassette and the volume was measured and results normalized. The concentration of TTR and AG10 obtained from the assay buffer were determined using NanoDrop and LCMS, respectively.

Selectivity of AG10 and Tafamidis to TTR Compared to Other Serum Proteins. The FPE assay was modified and performed with purified human TTRwt (5 μM). Other serum proteins were added either individually or in combination [fibrinogen (5 μM), albumin (600 μM), IgG (70 μM), transferrin (25 μM)] to the TTR and FPE mixture, and the fluorescence was monitored for 6 h as described above. The percentage of FPE probe binding to TTR in the presence of serum proteins measured after 3 h of incubation was used to calculate % TTR occupancy.

Seven-Day Repeat Oral Dosing of AG10 to Dogs. Sixteen male (M) and 16 female (F) beagle dogs, separated into four treatment groups and orally dosed by gavage with vehicle (6M/6F at 0 mg/kg) or AG10 in 0.5% methylcellulose formulation (2M/2F at 50 mg/kg, 2M/2F at 100 mg/kg, and 6M/6F at 200 mg/kg) for a total of 32 dogs. Blood (approximately 1.5 mL) was collected from a jugular vein into serum separator tubes on study day 1 (predose D1), predose study day 7 (predose D7), and at 1 h postdose study day 7 (postdose D7). These serum samples were analyzed for their TTR occupancy using the FPE assay described above.

Single Oral Doses of AG10 to Dogs to Determine an Exposure−Effect (PK−PD) Relationship with Respect to Binding to and Stabilization of TTR. Four male and four female beagle dogs, separated into two treatment groups (n = 2/sex/group) for a total of eight dogs were evaluated to acquire simultaneous pharmacokinetic (PK) and pharmacodynamic (PD) data for AG10 binding to and stabilization of TTR. Each animal received a single oral gavage (PO) of AG10 at a single dose of either 5 or 20 mg/kg in 0.5% methylcellulose. Blood was collected and analyzed predose and at 2, 4, 6, 8, 12, and 24 h postdose. The concentration of AG10 in these serum samples was analyzed by LCMS and the TTR occupancy by the FPE assay.

Statistical Analysis. All results are expressed as mean ± SD. All statistical analysis was performed with GraphPad PRISM software. The significance of the differences were measured by One-Way ANOVA followed by Tukey's multiple comparison test (n.s., not significant; $*p \leq 0.05$; $**p \leq 0.01$; $***p \leq 0.001$).

Chemistry: General. All reactions were carried out under argon atmosphere using dry solvents under anhydrous conditions unless otherwise noted. The solvents used were ACS grade from Fisher. Reagents were purchased from Aldrich and Fisher and used without further purification. Reactions were monitored by thin-layer chromatography (TLC) carried out on 0.20 mm POLYGRAM SIL silica gel plates (Art.-Nr. 805 023) with fluorescent indicator UV254 using UV light as a visualizing agent. Normal phase flash column chromatography was carried out using Davisil silica gel (100−200 mesh, Fisher). ^{1}H NMR and ^{13}C NMR spectra were recorded on a Jeol JNM-ECA600 spectrometer and calibrated using residual undeuterated solvent as an internal reference. Coupling constants (J) were expressed in hertz. The following abbreviations were used to explain the multiplicities: s = singlet, d = doublet, t = triplet, q = quartet, m = multiplet. High-resolution mass spectra (HRMS) were recorded by JEOL Direct Analysis in Real Time (DART) AccuTOF. HPLC analysis was performed on Agilent 1100 series HPLC system connected to a diode array detector operating between the UV ranges of 200−400 nm and quantified using Agilent Chemstation software. The HPLC analysis was performed on both Waters XBridge C18 column with L1 packing (4.6 mm × 250 mm, 5 μm) and SymmetricTM C4 (2.1 mm × 150 mm, 5 μm) at ambient temperature upon injection of a 50 μL of each blank buffer, standard, and/or sample to obtain the chromatogram. The mobile phase was composed of solvent A consisting methanol−water (5:95, v/v) containing 0.1% formic acid and solvent B consisting methanol−water (95:5, v/v) containing 0.1% formic acid. The HPLC program was a gradient separation method increasing linearly from 0% to 100%

DOI: 10.1021/acs.jmedchem.8b00817
J. Med. Chem. XXXX, XXX, XXX−XXX

solvent B from 0 to 20 min and then maintained 100% solvent B up to 30 min.

Key Compounds Purity. HPLC analysis was performed on both C18 and C4 reversed-phase columns. The purity for all key compounds was >95%. Description of the purity analysis has been included in the Experimental Section. Detailed HPLC information of key compounds (traces, retention times, and %purity) are included in the Supporting Information.

Synthetic Procedures. AG10 and tafamidis were synthesized as reported earlier.[15] Tolcapone and diflunisal were purchased from Fisher. All AG10 analogues were prepared as described below.

*3-(3-(3,5-Dimethyl-1H-pyrazol-4-yl)propoxy)-4-iodobenzoic Acid (**1**).* A solution of methyl 3-(3-bromopropoxy)-4-Iodobenzoate (**5a**)[15] (834 mg, 2.1 mmol, 1 equiv) in benzene (3 mL) was added dropwise to a solution of acetyl acetone (0.43 mL, 4.2 mmol, 2 equiv) and DBU (0.627 mL, 4.2 mmol, 2 equiv) in benzene (7 mL). The reaction mixture was stirred at room temperature for 3 days. The mixture was filtered and concentrated. To a solution of this intermediate in ethanol (5 mL) was added hydrazine hydrate (0.28 mL, 5.25 mmol, 2.5 equiv), and the reaction was heated under reflux for 4 h. The reaction was concentrated and purified by flash column chromatography (silica gel, 1−20% MeOH/CH_2Cl_2) to afford the methyl ester of compound **1**; sodium hydroxide (79 mg, 1.98 mmol, 2 equiv) in water (2.5 mL) was added to a solution of ester intermediate (412 mg, 0.99 mmol) in methanol (10 mL), and the reaction was heated under reflux for 4 h (50 °C). The reaction was concentrated and purified by flash column chromatography (silica gel, 1−5% MeOH/EtOAc) to afford compound **1** (183 mg, 22% yield for three steps); (98.3% purity by HPLC) t_R (column) (C18) = 25.72 min; t_R (C4) = 16.06 min. ^{1}H NMR (CD_3OD, 600 MHz) δ 7.86 (d, 1H, J = 8.4 Hz), 7.41 (d, 1H, J = 1.2 Hz), 7.34 (dd, 1H, J = 1.2 and 8.4 Hz), 4.0 (t, 2H, J = 6.0 Hz), 2.67 (t, 2H, J = 7.2 Hz), 2.13 (s, 6H), 1.97−1.93 (m, 2H). ^{13}C NMR (CD_3OD, 600 MHz) δ 168.5, 157.6, 142, 139.2, 133.2, 123.1, 114, 117.8, 91.7, 67.5, 29.6, 18.7, 9.3. HRMS (DART) m/z: calcd for $C_{15}H_{17}IN_2O_3$ + H^+ 401.0362; found 401.0347 (M + H^+).

*Methyl 3-(3-(3,5-Dimethyl-1H-pyrazol-4-yl)propoxy)-4-fluorobenzoate (**2**).* A solution of methyl 3-(3-bromopropoxy)-4-fluorobenzoate (**5b**)[15] (780 mg, 2.69 mmol, 1 equiv) in benzene (3 mL) was added dropwise to a solution of acetyl acetone (0.552 mL, 5.38 mmol, 2 equiv) and DBU (0.804 mL, 5.38 mmol, 2 equiv) in benzene (7 mL). The reaction mixture was stirred at room temperature for 3 days. The mixture was filtered and concentrated. The residue was purified by flash column chromatography (silica gel, 1−10% EtOAc/hexanes) to afford the alkylated intermediate which was used in the next step directly. To a solution of this intermediate in ethanol (5 mL) was added hydrazine hydrate (0.36 mL, 6.73 mmol, 2.5 equiv), and the reaction was heated under reflux for 4 h. The reaction was concentrated and purified by flash column chromatography (silica gel, 1−20% MeOH/CH_2Cl_2) to afford compound **2** (288 mg, 35% yield); (96.3% purity by HPLC) t_R (column) (C18) = 25.11 min; t_R (C4) = 14.03 min. ^{1}H NMR (CD_3OD, 600 MHz) δ 7.63−7.58 (m, 2H), 7.19−7.15 (m, 1H), 4.00 (t, 2H, J = 6.0 Hz), 3.86 (s, 3H), 2.58 (t, 2H, J = 7.2 Hz), 2.12 (s, 6H), 1.97−1.92 (m, 2H). ^{13}C NMR (CD_3OD, 600 MHz) δ 168.1, 158.4, 156.7, 148.9, 128.5, 124.6, 117.6, 117.0, 115.6, 69.4, 53.3, 31.1, 20.2, 10.9. HRMS (DART) m/z: calcd for $C_{16}H_{19}FN_2O_3$ + H^+ 307.1458, found 307.1463 (M + H^+).

*4-Fluoro-3-(3-(1,3,5-trimethyl-1H-pyrazol-4-yl)propoxy)benzoic Acid (**3**).* A solution of **2** (21 mg, 0.07 mmol, 1 equiv) in DMF (3 mL) was added sodium hydride (5 mg, 0.21 mmol, 3 equiv) and methyl iodide (17 μL, 0.28 mmol, 4 equiv). The reaction mixture was stirred at room temperature for 2 h. The mixture was extracted with brine, filtered, and concentrated. The residue was purified by flash column chromatography (silica gel, 0.5−2% MeOH/EtOAc) to afford the alkylated intermediate which was used in the next step directly. Sodium hydroxide (5.6 mg, 0.14 mmol, 2 equiv) in water (0.5 mL) was added to a solution of alkylated intermediate in methanol (2 mL), and the reaction was heated under reflux for 4 h (50 °C). The reaction was concentrated and purified by flash column chromatography (silica gel, 1−5% MeOH/EtOAc) to afford compound **3** (11 mg, 52% yield for two steps); (97.8% purity by HPLC) t_R (column) (C18) = 25.25 min; t_R (C4) = 15.71 min. ^{1}H NMR (CD_3OD, 600 MHz) δ 7.58−7.51 (m, 2H), 7.10−7.06 (m, 1H), 3.92 (t, 2H, J = 6.0 Hz), 3.56 (s, 3H), 2.49 (t, 2H, J = 7.2 Hz), 2.05 (s, 3H), 2.01 (s, 3H), 1.83−1.88 (m, 2H). ^{13}C NMR (CD_3OD, 600 MHz) δ 168.1, 154.6, 146.8, 145.3, 137.2, 128.1, 122.8, 115.5, 115.4, 114.8, 67.4, 34.3, 29.4, 18.8, 10.1, 7.9. HRMS (DART) m/z: calcd for $C_{16}H_{19}FN_2O_3$ + H^+ 307.1458, found 307.1449 (M + H^+).

*3-(3-(3,5-Diethyl-1H-pyrazol-4-yl)propoxy)-4-fluorobenzoic Acid (**4**).* Sodium hydroxide (3.2 mg, 0.08 mmol, 2 equiv) in water (0.5 mL) was added to a solution of **6** (13 mg, 0.04 mmol, 1 equiv) in methanol (2 mL), and the reaction was heated under reflux for 4 h (50 °C). The reaction was concentrated and purified by flash column chromatography (silica gel, 1−5% MeOH/EtOAc) to afford compound **4** (10 mg, 80% yield); (96.0% purity by HPLC) t_R (column) (C18) = 25.16 min; t_R (C4) = 15.56 min. ^{1}H NMR (CD_3OD, 600 MHz) δ 7.57−7.49 (m, 2H), 7.08−7.04 (m, 1H), 3.94 (t, 2H, J = 6.0 Hz), 2.51−2.43 (m, 6H), 1.87−1.82 (m, 2H), 1.06 (t, 6H, J = 7.8 Hz). ^{13}C NMR (CD_3OD, 600 MHz) δ 169.8, 157.9, 156.3, 149.3, 148.5, 124.6, 117.2, 117.1, 114.1, 69.4, 31.8, 20.1, 19.9, 14.7. HRMS (DART) m/z: calcd for $C_{17}H_{21}FN_2O_3$ + H^+ 321.1614, found 321.1601 (M + H^+).

*Methyl 3-(3-Bromopropoxy)-4-fluorobenzoate (**5**).* Compound **5** was synthesized as reported earlier.[15] To a solution of methyl 4-fluoro-3hydroxybenzoate (1.0 g, 5.87 mmol, 1 equiv) and 1,3-dibromopropane (3.0 mL, 29.4 mmol, 5 equiv) in DMF (15 mL) was added K_2CO_3 (0.98 g, 7.1 mmol, 1.2 equiv). The reaction mixture was stirred at room temperature for 16 h. The mixture was diluted with EtOAc (500 mL), washed with brine (3 × 200 mL), and dried with Na_2SO_4. The solution was filtered and concentrated. The residue was purified by flash column chromatography (silica gel, 1−10% EtOAc/hexanes) to afford compound **5** (1.3 g, 76% yield). ^{1}H NMR (CD_3OD, 600 MHz) δ 7.67−7.61 (m, 2H), 7.14−7.07 (m, 1H), 4.21 (t, 2H, J = 5.89 Hz), 3.89 (s, 3H), 3.62 (t, 2H, J = 6.38 Hz), 2.38−2.31 (m, 2H). ESI+ m/z: calcd for $C_{11}H_{12}BrFO_3$ + H^+ 290.00, found 290.01 (M + H^+).

*Methyl 3-(3-(3,5-Diethyl-1H-pyrazol-4-yl)propoxy)-4-fluorobenzoate (**6**).* A solution of **5b** (100 mg, 0.35 mmol, 1 equiv) in benzene (2 mL) was added dropwise to a solution of 3,5-heptanedione (0.095 mL, 0.7 mmol, 2 equiv) and DBU (0.104 mL, 0.7 mmol, 2 equiv) in benzene (5 mL). The reaction mixture was stirred at room temperature for 3 days. The mixture was filtered and concentrated. The residue was purified by flash column chromatography (silica gel, 1−10% EtOAc/hexanes) to afford the alkylated intermediate which was used in the next step directly. Hydrazine hydrate (0.047 mL, 0.875 mmol, 2.5 equiv) was added to the alkylated intermediate in ethanol (4 mL), and the reaction was heated under reflux for 4 h. The reaction was concentrated and purified by flash column chromatography (silica gel, 1−5% MeOH/EtOAc) to afford compound **6** (75 mg, 65% yield for two steps). ^{1}H NMR (CD_3OD, 600 MHz) δ 7.59−7.54 (m, 2H), 7.15−7.11 (m, 1H), 3.98 (t, 2H, J = 6.0 Hz), 3.81 (s, 3H), 2.56−2.47 (m, 6H), 1.91−1.86 (m, 2H), 1.13 (t, 6H, J = 7.8 Hz). ^{13}C NMR (CD_3OD, 600 MHz) δ 167.9, 156.6, 156.2, 148.8, 148.7, 124.4, 117.5, 117.3, 116.9, 113.9, 69.5, 53.1, 31.8, 20.1, 14.7. HRMS (DART) m/z: calcd for $C_{18}H_{23}FN_2O_3$ + H^+ 335.1771, found 335.1773 (M + H^+).

■ ASSOCIATED CONTENT

Supporting Information

The Supporting Information is available free of charge on the ACS Publications website at DOI: 10.1021/acs.jmedchem.8b00817.

O−O distances between Ser117 residues in the tetrameric TTR complexes; chemical structure, ^{1}H NMR, and HRMS mass spectrometry data for FPE probe; Yasuda−Shedlovsky extrapolation curve for pKa calculation of AG10; efficacy of stabilizers in stabilizing

DOI: 10.1021/acs.jmedchem.8b00817
J. Med. Chem. XXXX, XXX, XXX−XXX

TTR in human serum in urea buffer; concentration−effect relationship for TTR occupancy by AG10 and tafamidis in whole human serum; correlation between TTR occupancy and TTR stabilization for AG10 and tafamidis; determination of TTR concentration in dog serum; data used to generate the PK−PD scatterplot in Figure 7c,d; HPLC analysis of AG10, tafamidis, diflunisal, tolcapone, and AG10 analogues **1**, **2**, **3**, and **4** (PDF)

Molecular formula strings of key compounds (CSV)

AUTHOR INFORMATION

Corresponding Authors

*For M.A.: E-mail, malhamadsheh@pacific.edu. Phone: +1-209-946-3164.

*For U.S.: E-mail, usinha@eidostx.com. Phone: +1-415-887-1471.

ORCID

Mamoun Alhamadsheh: 0000-0003-4325-7044

Author Contributions

M.M., A.P., and W.B. contributed equally, and U.S. and M.A. are considered senior authors.

Notes

The authors declare the following competing financial interest(s): Authors M.A. and I.G. are cofounders of Eidos Therapeutics. R.Z, N.K., J.F., and U.S. are employees of Eidos Therapeutics. The remaining authors declare noncompeting financial interests.

ACKNOWLEDGMENTS

This work was supported by the National Institutes of Health grant 1R15GM110677-01 (M.A.) and Eidos Therapeutics. The support by a National Science Foundation Instrumentation grant (NSF-MRI-0722654) is gratefully acknowledged. Thanks to Vyacheslav Samoshin and Andreas Franz for NMR and mass spectrometric analysis.

ABBREVIATIONS USED

TTR, transthyretin; ATTR, transthyretin amyloidosis; ATTR-CM, transthyretin amyloid cardiomyopathy; TTRm, transthyretin mutations; TTRwt, wild-type transthyretin; ATTRm-CM, familial transthyretin amyloid cardiomyopathy; ATTRwt-CM, wild-type transthyretin amyloid cardiomyopathy; ATTR-PN, transthyretin peripheral polyneuropathy; T4, thyroxine; ITC, isothermal titration calorimetry; NSAIDs, nonsteroidal anti-inflammatory drugs; FPE assay, fluorescence probe exclusion assay; PK-PD, pharmacokinetic−pharmacodynamic

REFERENCES

(1) Falk, R. H.; Comenzo, R. L.; Skinner, M. The systemic amyloidoses. *N. Engl. J. Med.* **1997**, *337*, 898−909.

(2) Johnson, S. M.; Wiseman, R. L.; Sekijima, Y.; Green, N. S.; Adamski-Werner, S. L.; Kelly, J. W. Native state kinetic stabilization as a strategy to ameliorate protein misfolding diseases: a focus on the transthyretin amyloidoses. *Acc. Chem. Res.* **2005**, *38*, 911−921.

(3) Brunjes, D. L.; Castano, A.; Clemons, A.; Rubin, J.; Maurer, M. S. Transthyretin cardiac amyloidosis in older Americans. *J. Card. Failure* **2016**, *22*, 996−1003.

(4) Ton, V. K.; Mukherjee, M.; Judge, D. P. Transthyretin cardiac amyloidosis: pathogenesis, treatments, and emerging role in heart failure with preserved ejection fraction. *Clin. Med. Insights: Cardiol.* **2014**, *8s1*, 39−44.

(5) Buxbaum, J. N.; Ruberg, F. L. Transthyretin V122I (pV142I)* cardiac amyloidosis: an age-dependent autosomal dominant cardiomyopathy too common to be overlooked as a cause of significant heart disease in elderly African Americans. *Genet. Med.* **2017**, *19*, 733−742.

(6) Alexander, K. M.; Falk, R. H. V122I TTR cardiac amyloidosis in patients of African descent: recognizing a missed disease or the dog that didn't bark? *Circ.: Heart Failure* **2016**, *9*, e003489.

(7) Connors, L. H.; Doros, G.; Sam, F.; Badiee, A.; Seldin, D. C.; Skinner, M. Clinical features and survival in senile systemic amyloidosis: comparison to familial transthyretin cardiomyopathy. *Amyloid* **2011**, *18*, 157−159.

(8) Connors, L. H.; Lim, A.; Prokaeva, T.; Roskens, V. A.; Costello, C. E. Tabulation of human transthyretin (TTR) variants, 2003. *Amyloid* **2003**, *10*, 160−184.

(9) Hammarström, P.; Jiang, X.; Hurshman, A. R.; Powers, E. T.; Kelly, J. W. Sequence-dependent denaturation energetics: a major determinant in amyloid disease diversity. *Proc. Natl. Acad. Sci. U. S. A.* **2002**, *99*, 16427−16432.

(10) Adams, D.; Théaudin, M.; Cauquil, C.; Algalarrondo, V.; Slama, M. FAP neuropathy and emerging treatments. *Curr. Neurol. Neurosci. Rep.* **2014**, *14*, 435.

(11) Sekijima, Y.; Dendle, M. T.; Wiseman, R. L.; White, J. T.; D'Haeze, W.; Kelly, J. W. R104H may suppress transthyretin amyloidogenesis by thermodynamic stabilization, but not by the kinetic mechanism characterizing T119 interallelic trans-suppression. *Amyloid* **2006**, *13*, 57−66.

(12) Coelho, T.; Chorão, R.; Sousa, R.; Alves, I.; Torres, M. F.; Saraiva, M. Compound heterozygotes of transthyretin Met30 and transthyretin Met119 are protected from the devastating effects of familial amyloid polyneuropathy. *Neuromuscul Disord* **1996**, *6*, S20.

(13) Hornstrup, L. S.; Frikke-Schmidt, R.; Nordestgaard, B. G.; Tybjærg-Hansen, A. Genetic stabilization of transthyretin, cerebrovascular disease, and life expectancy. *Arterioscler., Thromb., Vasc. Biol.* **2013**, *33*, 1441−1447.

(14) Terazaki, H.; Ando, Y.; Misumi, S.; Nakamura, M.; Ando, E.; Matsunaga, N.; Shoji, S.; Okuyama, M.; Ideta, H.; Nakagawa, K.; Ishizaki, T.; Ando, M.; Saraiva, M. J. A novel compound heterozygote (FAP ATTR Arg104His/ATTR Val30Met) with high serum transthyretin (TTR) and retinol binding protein (RBP) levels. *Biochem. Biophys. Res. Commun.* **1999**, *264*, 365−370.

(15) Penchala, S. C.; Connelly, S.; Wang, Y.; Park, M. S.; Zhao, L.; Baranczak, A.; Rappley, I.; Vogel, H.; Liedtke, M.; Witteles, R. M.; Powers, E. T.; Reixach, N.; Chan, W. K.; Wilson, I. A.; Kelly, J. W.; Graef, I. A.; Alhamadsheh, M. M. AG10 inhibits amyloidogenesis and cellular toxicity of the familial amyloid cardiomyopathy-associated V122I transthyretin. *Proc. Natl. Acad. Sci. U. S. A.* **2013**, *110*, 9992−9997.

(16) Iakovleva, I.; Brännström, K.; Nilsson, L.; Gharibyan, A. L.; Begum, A.; Anan, I.; Walfridsson, M.; Sauer-Eriksson, A. E.; Olofsson, A. Enthalpic forces correlate with the selectivity of transthyretin-stabilizing ligands in human plasma. *J. Med. Chem.* **2015**, *58*, 6507−6515.

(17) Freire, E. Do enthalpy and entropy distinguish first in class from best in class? *Drug Discovery Today* **2008**, *13*, 869−874.

(18) Choi, S.; Kelly, J. W. A competition assay to identify amyloidogenesis inhibitors by monitoring the fluorescence emitted by the covalent attachment of a stilbene derivative to transthyretin. *Bioorg. Med. Chem.* **2011**, *19*, 1505−1514.

(19) Bulawa, C. E.; Connelly, S.; Devit, M.; Wang, L.; Weigel, C.; Fleming, J. A.; Packman, J.; Powers, E. T.; Wiseman, R. L.; Foss, T. R.; Wilson, I. A.; Kelly, J. W.; Labaudinière, R. Tafamidis, a potent and selective transthyretin kinetic stabilizer that inhibits the amyloid cascade. *Proc. Natl. Acad. Sci. U. S. A.* **2012**, *109*, 9629−9634.

(20) Sant'Anna, R.; Gallego, P.; Robinson, L. Z.; Pereira-Henriques, A.; Ferreira, N.; Pinheiro, F.; Esperante, S.; Pallares, I.; Huertas, O.; Almeida, M. R.; Reixach, N.; Insa, R.; Velazquez-Campoy, A.; Reverter, D.; Reig, N.; Ventura, S. Repositioning tolcapone as a

DOI: 10.1021/acs.jmedchem.8b00817
J. Med. Chem. XXXX, XXX, XXX−XXX

potent inhibitor of transthyretin amyloidogenesis and associated cellular toxicity. *Nat. Commun.* **2016**, *7*, 10787 1−13.
(21) Adamski-Werner, S. L.; Palaninathan, S. K.; Sacchettini, J. C.; Kelly, J. W. Diflunisal analogues stabilize the native state of transthyretin, potent inhibition of amyloidogenesis. *J. Med. Chem.* **2004**, *47*, 355−374.
(22) Sebastião, M. P.; Lamzin, V.; Saraiva, M. J.; Damas, A. M. Transthyretin stability as a key factor in amyloidogenesis: x-ray analysis at atomic resolution. *J. Mol. Biol.* **2001**, *306*, 733−744.
(23) Kim, J. H.; Oroz, J.; Zweckstetter, M. Structure of monomeric transthyretin carrying the clinically important T119M mutation. *Angew. Chem., Int. Ed.* **2016**, *55*, 16168−16171.
(24) Morais-de-Sá, E.; Pereira, P. J.; Saraiva, M. J.; Damas, A. M. The crystal structure of transthyretin in complex with diethylstilbestrol: a promising template for the design of amyloid inhibitors. *J. Biol. Chem.* **2004**, *279*, 53483−53490.
(25) Ortore, G.; Orlandini, E.; Braca, A.; Ciccone, L.; Rossello, A.; Martinelli, A.; Nencetti, S. Targeting different transthyretin binding sites with unusual natural compounds. *ChemMedChem* **2016**, *11*, 1865−1874.
(26) Lima, L. M.; Silva, V. e. A.; Palmieri, L. e. C.; Oliveira, M. C.; Foguel, D.; Polikarpov, I. Identification of a novel ligand binding motif in the transthyretin channel. *Bioorg. Med. Chem.* **2010**, *18*, 100−110.
(27) Neto-Silva, R. M.; Macedo-Ribeiro, S.; Pereira, P. J.; Coll, M.; Saraiva, M. J.; Damas, A. M. X-ray crystallographic studies of two transthyretin variants: further insights into amyloidogenesis. *Acta Crystallogr., Sect. D: Biol. Crystallogr.* **2005**, *61*, 333−339.
(28) Fex, G.; Laurell, C. B.; Thulin, E. Purification of prealbumin from human and canine serum using a two-step affinity chromatographic procedure. *Eur. J. Biochem.* **1977**, *75*, 181−186.
(29) Klebe, G. Applying thermodynamic profiling in lead finding and optimization. *Nat. Rev. Drug Discovery* **2015**, *14*, 95−110.
(30) Ross, P. D.; Subramanian, S. Thermodynamics of protein association reactions: forces contributing to stability. *Biochemistry* **1981**, *20*, 3096−3102.
(31) Sergeev, Y. V.; Dolinska, M. B.; Wingfield, P. T. Thermodynamic analysis of weak protein interactions using sedimentation equilibrium. *Curr. Protoc. Protein Sci.* **2014**, *77*, 20.13.1−20.13.15.
(32) Dolinska, M. B.; Wingfield, P. T.; Sergeev, Y. V. βB1-Crystallin: thermodynamic profiles of molecular interactions. *PLoS One* **2012**, *7*, e29227.
(33) Vicart, P.; Caron, A.; Guicheney, P.; Li, Z.; Prévost, M. C.; Faure, A.; Chateau, D.; Chapon, F.; Tomé, F.; Dupret, J. M.; Paulin, D.; Fardeau, M. A missense mutation in the alphab-Crystallin chaperone gene causes a desmin-related myopathy. *Nat. Genet.* **1998**, *20*, 92−95.
(34) Arrar, M.; de Oliveira, C. A.; McCammon, J. A. Inactivating mutation in histone deacetylase 3 stabilizes its active conformation. *Protein Sci.* **2013**, *22*, 1306−1312.
(35) Bartels, T.; Choi, J. G.; Selkoe, D. J. α-Synuclein occurs physiologically as a helically folded tetramer that resists aggregation. *Nature* **2011**, *477*, 107−110.
(36) Makley, L. N.; McMenimen, K. A.; DeVree, B. T.; Goldman, J. W.; McGlasson, B. N.; Rajagopal, P.; Dunyak, B. M.; McQuade, T. J.; Thompson, A. D.; Sunahara, R.; Klevit, R. E.; Andley, U. P.; Gestwicki, J. E. Pharmacological chaperone for α-Crystallin partially restores transparency in cataract models. *Science* **2015**, *350*, 674−677.
(37) Sekijima, Y.; Dendle, M. A.; Kelly, J. W. Orally administered diflunisal stabilizes transthyretin against dissociation required for amyloidogenesis. *Amyloid* **2006**, *13*, 236−249.
(38) Schaftenaar, G.; Noordik, J. H. Molden: a pre- and post-processing program for molecular and electronic structures. *J. Comput.-Aided Mol. Des.* **2000**, *14*, 123−134.
(39) Pettersen, E. F.; Goddard, T. D.; Huang, C. C.; Couch, G. S.; Greenblatt, D. M.; Meng, E. C.; Ferrin, T. E. UCSF chimera–a visualization system for exploratory research and analysis. *J. Comput. Chem.* **2004**, *25*, 1605−1612.

DOI: 10.1021/acs.jmedchem.8b00817
J. Med. Chem. XXXX, XXX, XXX−XXX